

## High genetic diversity and limited regional population differentiation in populations of *Calonectria pseudoreteaudii* from *Eucalyptus* plantations

WenWen Li<sup>a,b,d</sup>, FeiFei Liu<sup>b,c,d</sup>, ShuaiFei Chen<sup>b,c,†</sup>, Michael J. Wingfield<sup>c</sup>, Tuan A. Duong<sup>c</sup>

<sup>a</sup> Department of Plant and Soil Sciences, Forestry and Agricultural Biotechnology Institute (FABI), University of Pretoria, Pretoria 0028, South Africa

<sup>b</sup> Research Institute of Fast-growing Trees (RIFT), Chinese Academy of Forestry (CAF), ZhanJiang 524022, GuangDong Province, China

<sup>c</sup> Department of Biochemistry, Genetics and Microbiology, Forestry and Agricultural Biotechnology Institute (FABI), University of Pretoria, Pretoria 0028, South Africa

<sup>d</sup> These authors contributed equally to this work.

<sup>†</sup> Corresponding author: S. F. Chen, shuaifei.chen@gmail.com

### Abstract

*Calonectria pseudoreteaudii* causes a serious and widespread disease known as *Calonectria* leaf blight in *Eucalyptus* plantations of southern China. Little is known regarding the population biology or reproductive biology of this pathogen in the affected areas. The aims of this study were to investigate the genetic diversity, population structure and the reproductive mode of *C. pseudoreteaudii* from affected *Eucalyptus* plantations of southern China. Ten polymorphic SSR markers were developed for the species, and were used to genotype 311 isolates from eight populations. The mating types of all isolates were identified using the *MAT* gene primers. The results revealed a high level of genetic diversity of the pathogen in all investigated populations. Of the 90 multilocus genotypes detected, ten were shared between at least two populations. With the exception of one population from HuiZhou, GuangDong (7HZ), the most dominant genotype was shared in seven remaining populations. DAPC and population differentiation analyses showed that the 7HZ population was well differentiated from the others and that there was no significant differentiation between the remaining populations. AMOVA suggested that most molecular

variation was within populations (86%). Index of association analysis was consistent with a predominantly asexual life cycle for *C. pseudoreteaudii* in the studied regions. Although both mating types were detected in seven of the eight populations, the *MAT1-1/MAT1-2* ratios in these populations deviated significantly from the 1:1 ratio expected in a randomly mating population.

**Keywords:** genetic diversity, plant pathogen, population structure, reproduction mode

## 1. Introduction

The growing demand for timber and *Eucalyptus*-derived products has led to the rapid expansion of *Eucalyptus* plantation areas in China and worldwide (Burgess and Wingfield 2017; Xie et al. 2017). The accompanying disease problems caused by pests and pathogens pose a great threat to the health of *Eucalyptus* plantations (Wingfield et al. 2015). Human activities, such as trade of germplasm, are key drivers promoting the movement of pathogens between regions (Wingfield et al. 2008). This also has a significant impact on pathogen evolution in favor of higher genetic diversity in invaded areas (McDonald and Linde 2002; Wingfield et al. 2015).

*Calonectria* leaf blight (CLB) is one of the most destructive foliar diseases of *Eucalyptus* in plantations. In recent years, frequent CLB outbreaks have occurred in plantations of southern China (Li et al. 2023b; Liang et al. 2023; Wang and Chen 2020; Wu and Chen 2021). The disease mainly occurs in one- to two-year-old plantations, characterized by small round gray to brown spots that extend throughout the leaves, resulting in leaf blight and defoliation (Crous 2002; Old et al. 2003). This affects growth due to the reduction in photosynthetic area, eventually leading to timber yield loss (Crous et al. 2019). According to incomplete estimates, *Calonectria* leaf blight causes a loss in annual *Eucalyptus* growth rates of up to 32% in GuangXi Province, resulting in an economic loss of nearly 4 million CNY (Zhou 2020). In Fujian Province, the annual economic loss can reach 58 million CNY (Zhu et al. 2011). Many *Calonectria* species have been shown to cause CLB in *Eucalyptus* (Chen et al. 2011; Freitas et al. 2019; Li et al. 2023a; Liang et al. 2023), of which *C. pseudoreteaudii* is the most common and aggressive species in southern China (Li et al. 2023b; Liang et al. 2023; Wang and Chen 2020; Wu and Chen 2021).

*Calonectria pseudoreteaudii* was first discovered in 2010 on stems of *E. urophylla* × *E. grandis* hybrid cuttings in a nursery in GuangDong Province (Lombard et al. 2010). It has subsequently been found to cause serious disease in many *Eucalyptus* plantations and nurseries of FuJian,

GuangDong, GuangXi and HaiNan Provinces (Li et al. 2017; Liang et al. 2023; Liu et al. 2022; Wu and Chen 2021). In addition to *Eucalyptus* trees, this pathogen infects *Macadamia spp.* in YunNan Province, causing fruit spot (Jiang et al. 2020), and *Vaccinium corymbosum* in GuangDong Province, causing leaf spot and stem blight (Chen et al. 2023). *C. pseudoreteaudii* has also been reported on *Eucalyptus* and *Macadamia* in India, Laos, and Vietnam (Bose et al. 2022; Crous et al. 2012; Phanthavong et al. 2023).

*C. pseudoreteaudii* has a heterothallic mating system (Li et al. 2020; Wu and Chen 2021), which requires two individuals of opposite mating types for sexual reproduction to occur (Coppin et al. 1997). However, sexual morphs of *C. pseudoreteaudii* have never been found in nature, despite both mating types occurring in natural populations (Li et al. 2023a; Wu and Chen 2021). An important factor when considering population biology of fungi is that the absence of sexual morphs does not preclude the potential for sexual recombination (Billiard et al. 2012; Goodenough and Heitman 2014). Therefore, the possibility exists that more aggressive genotypes could be generated through sexual reproduction in the *C. pseudoreteaudii* populations (Li et al. 2022).

Understanding the population dynamics and reproductive biology of pathogens is important when considering disease management options. However, most studies on *C. pseudoreteaudii* have focused on its taxonomy, occurrence, and pathogenicity (Li et al. 2017; Liang et al. 2023; Wang and Chen 2020; Wu and Chen 2021) with little attention paid to the population biology of the pathogen. There has been only a single population genetic study on *C. pseudoreteaudii* showing that the fungus in the soil may have originated from infections on diseased *Eucalyptus* trees (Wu et al. 2023). The aims of the present study were to assess the genetic diversity and population structure of *C. pseudoreteaudii* from *Eucalyptus* plantations in southern China using SSR markers. Furthermore, to consider the mating type distribution in populations so as to understand the mode of reproduction of the pathogen associated with disease outbreaks.

## **2. Materials and methods**

### **2.1 Fungal isolates, DNA extraction and confirmation of identity**

A total of 311 *C. pseudoreteaudii* isolates from diseased *Eucalyptus* leaves representing eight geographic regions in three provinces of southern China were used in this study (Fig. 1, Supplementary Table S1). Of these, data for 64 isolates from BeiHai (1BH) region have previously

been published (Wu and Chen 2021; Wu et al. 2023), four isolates from LeiZhou, ZhanJiang (2ZJA) and two isolates from MaZhang, ZhanJiang (3ZJB) were collected and identified by Wang and Chen (2020), 42 isolates from YangJiang (4YJ), 48 isolates from QingYuan (5QY), 36 isolates from JiangMen (6JM) and 36 isolates from HuiZhou (7HZ) regions were collected and identified by Li et al. (2023b), and eight of the 23 isolates from HaiNan (8HN) were collected and identified by Liang et al. (2023). The remaining 15 isolates from 8HN, 28 isolates from 2ZJA and 28 isolates from 3ZJB regions were identified as part of the present study. All isolates have been maintained in the culture collection (CSF) of Research Institute of Fast-growing Trees (RIFT) of the Chinese Academy of Forestry (CAF) in ZhanJiang, GuangDong Province, China.

For the newly collected isolates, single conidial cultures were transferred to 2% malt extract agar (MEA) plates to ensure that each culture was derived from a single individual. Mycelium was scraped from the surface of 5- to 7-day-old cultures, and DNA was extracted using the CTAB method described by van Burik et al. (1998). The final concentration of DNA was adjusted to approximately 100 ng/uL using ddH<sub>2</sub>O.

The translation elongation factor 1-alpha (*tef1*) and  $\beta$ -tubulin (*tub2*) regions were amplified and sequenced to confirm the identity of isolates. Primers EF1-728F (5'-CATCGAGAAGTTCGAGAAGG-3', Carbone and Kohn 1999) and EF2 (5'-GGARGTACCAGTSATCATGTT-3', O'Donnell et al. 1998) were used to amplify and sequence the *tef1* and the primers T1 (5'-AACATGCGTGAGATTGTAAGT-3', O'Donnell and Cigelnik 1997) and CYLTUB1R (5'-AGTTGTCGGGACGGAAGAG-3', Crous et al. 2004) were used for *tub2*. The PCR reaction mixture consisted of 17.5  $\mu$ L TopTaq™ Master Mix, 2  $\mu$ L DNA samples, 1  $\mu$ L of each primer and nuclease-free H<sub>2</sub>O to a final volume of 35  $\mu$ L (Liu et al. 2020). The thermal cycle was as follows: an initial denaturation step at 95 °C for 5 min; followed by 35 cycles of [95 °C for 30 s; annealing at 52 °C for 30 s; 72 °C for 1 min], and the final extension step at 72 °C for 10 min (Liu et al. 2020). PCR products were sequenced in both directions by the Beijing Genomics Institute (BGI, GuangZhou, China).

The sequences obtained were curated, and consensus sequences were derived using Geneious v.9.1.4 (Kearse et al. 2012). All sequences were aligned using an online instance of MAFFT v.7

(Kato and Standley 2013), and each representing a different haplotype based on *tefl* and *tub2* was selected to produce a maximum likelihood (ML) phylogenetic tree using PhyML v. 3.0 (Guindon and Gascuel 2003). Only those isolates identified as *C. pseudoreteaudii* were used in the population genetic analyses.

## 2.2 SSR maker development

Genome data from three isolates of *C. pseudoreteaudii* were utilized for the development of SSR markers. This dataset included a high-quality reference genome sequence from the *C. pseudoreteaudii* isolate CSF13040 (NCBI accession number: JBDIVA000000000) and unassembled genomic data from two additional isolates, CSF10059 and CSF13337. Isolate CSF10059 was obtained from soil in a *Eucalyptus* plantation in Fujian Province, while CSF13337 was collected from a diseased *Eucalyptus* tree on the Leizhou Peninsula, Zhanjiang, Guangdong Province. Genomic DNA was extracted following the protocol of Duong et al. (2013). Illumina sequencing was performed by Macrogen (Seoul, South Korea) using the Illumina HiSeq2500 platform to produce 251 bp paired-end reads. Quality control of the raw sequencing data was conducted using FastQC v0.11.5 (Afgan et al. 2016), and adapter trimming was performed with Trimmomatic v0.36 (Bolger et al. 2014).

The pipeline described in Engelbrecht et al. (2017) was used to develop SSR markers. Briefly, the SSRs were identified from the reference genome (isolate CSF13040) using the REPET package (Flutre et al., 2011). Only tri- and tetra-nucleotide repeats identified by REPET were considered for SSR development. These repeats were cataloged into an SSR region file for subsequent SSR genotyping. The trimmed reads from isolates CSF10059 and CSF13337 were aligned to the reference genome using Bowtie2 (Langmead and Salzberg 2012) to generate BAM files. RepeatSeq v0.8.2 (Highnam et al. 2013) was used to genotype the SSR markers included in the region file with BAM alignments as inputs. The polymorphic SSR markers identified between the reference genome and CSF10059 and/or CSF13337 isolates, along with 500 bp upstream and downstream flanking sequences, were extracted from the reference genome for further analysis.

To ensure primer specificity, local BLAST searches of the extracted SSRs with their flanking regions against the reference genome were conducted. Based on the BLAST results, only those with a single genomic location were retained for primer design. Primer design was carried out using Qiagen CLC Main Workbench 23 (<https://digitalinsights.qiagen.com/>), with parameters set for

fragment sizes between 150 and 500 bp and an annealing temperature of 48–58 °C.

Twelve *C. pseudoreteaudii* isolates from various regions were used to test the designed primers for PCR amplification and specificity. The amplification reactions were conducted as follows: an initial denaturation at 95°C for 5 min, followed by 35 cycles of 95°C for 30 s, annealing at 52°C for 30 s, 72°C for 1 min, and a final extension at 72°C for 10 min. The PCR reaction mixture, sequencing, sequence editing, and analysis parameters were similar to those used to amplify the *tef1* and *tub2* gene regions. The primer pairs that resulted in specific amplification of the targeted regions and had similar annealing temperature across different pairs were selected for genotyping the populations.

### **2.3 SSR genotyping**

PCR genotyping was performed for *C. pseudoreteaudii* isolates using the conditions stated above. To facilitate accurate scoring of the alleles, amplified SSR regions from all isolates were subjected to traditional Sanger sequencing. Sequences were assembled and aligned in Geneious v.9.1.4 (Kearse et al. 2012). Different sequence lengths observed at each locus, due to the variation in the number of repeat motifs, were considered different alleles. The combination of alleles generated by all primers for each isolate was defined as a multilocus genotype (MLG). A genotype accumulation curve generated in R (Kamvar et al. 2014) was used to assess whether the number of SSR primers was sufficient to capture the MLG diversity in populations.

### **2.4 Genetic diversity**

Eight populations were defined based on the geographical origin of the isolates, and these were used to calculate genetic diversity estimates. GenAlex v. 6.5 (Peakall and Smouse 2012) was used to assess the total number of alleles ( $N_a$ ), the number of effective alleles ( $N_{ef}$ ), and the number of MLGs. The unbiased gene diversity ( $H_{exp}$ ), evenness ( $E_5$ ), the number of expected MLGs at the smallest sample size based on rarefaction (eMLG), the Shannon-Wiener Index ( $H$ ) and Stoddart and Taylor's Index ( $G$ ) of MLG diversity were calculated using the R package poppr (Kamvar et al. 2014).

### **2.5 Genetic differentiation**

Analysis of molecular variance (AMOVA) was used to test the genetic variance among and within

populations based on geographic origin using GenAIEx v. 6.5 (Peakall and Smouse 2012). The significance level of genetic difference was tested based on 999 random permutations using the Monte Carlo test. Population differentiation ( $\phi_{PT}$ ) and gene flow ( $N_m$ ) were calculated for each pairwise comparison based on Nei's genetic distance with 999 permutations (Peakall and Smouse 2012).

## 2.6 Population structure

The software package STRUCTURE v. 2.3.3 was used to estimate the most probable number of genetic clusters ( $K$ ) and to assign individuals to specific sub-populations using a Bayesian clustering algorithm (Falush et al. 2003; Pritchard et al. 2000). The parameters were set to 20 independent runs for each  $K$ -value ( $K = 1-10$ ), with 250000 initial burn-in iterations followed by 1000000 MCMC iterations. The optimal  $K$ -value was identified using STRUCTURE HARVESTER (Earl and vonHoldt 2012). The structure bar plot was visualized using CLUMPAK (Kopelman et al. 2015). To further investigate the genetic clustering of *C. pseudoreteaudii* isolates, discriminant analysis of principal components (DAPC) was conducted using the R package adegenet (Jombart et al. 2010). The function xvalDAPC was used to confirm the optimal number of principal components (PCs) retained for each analysis, and 1000 replicates were executed at each level of PC retention.

## 2.7 Reproductive mode

To test the possibility of sexual recombination, index of association ( $I_a$ ) and standardized index of association ( $\bar{r}_d$ ) were calculated based on a clone corrected dataset using the ia function of the R package poppr (Kamvar et al. 2014). The null hypothesis was that alleles observed at different loci had no linkage. The significance ( $P$ -values) of  $I_a$  and  $\bar{r}_d$  tests were calculated with 999 permutations.

The mating types of all isolates were identified using the *MAT* genes primers and PCR amplification protocols described by Li et al. (2020). An exact binomial test (two-tailed) was used in R v.3.6.1 to determine whether the frequency of *MAT1-1* and *MAT1-2* observed in each population deviated significantly from the 1:1 ratio expected from a sexually random recombining population.

## 3. Results

### 3.1 Fungal isolates

A total of 311 isolates identified as *C. pseudoreteaudii* based on *tef1* and *tub2* gene regions were used in this study (Supplementary Table S1). The number of isolates per geographic population was 1BH (n = 64), 2ZJA (n = 32), 3ZJB (n = 30), 4YJ (n = 42), 5QY (n = 48), 6JM (n = 36), 7HZ (n = 36) and 8HN (n = 23) (Fig. 1).

### 3.2 SSR markers development and selection

Analysis of microsatellite repeats in the genome of isolate CSF13040 identified a total of 367 tri- and 125 tetra- nucleotide repeats. The Illumina sequence data of CSF10059 and CSF13337 were mapped to the reference genome to identify polymorphic SSRs. A total of 100 and 76 polymorphic SSR regions were retained from these two genomes, respectively. After further filtering for sequence complexity, 67 SSRs were considered for final marker development. A total of 38 primer pairs (Supplementary Table S2) were retained after filtering based on their having specific binding sites. PCR validation of these 38 markers resulted in 10 polymorphic markers that could be amplified with a high level of consistency and specificity. The sequences and properties of these primers are provided in Table 1.

### 3.3 SSR genotyping of *C. pseudoreteaudii* isolates

The targeted SSR regions were amplified in 311 isolates using the ten selected markers, except for three isolates that failed to sequence at three loci (CSF12369 at CPS103, CSF12296 at CPS159, CSF21543 at CPS115), respectively. A total of 92 alleles were detected among the 311 isolates across ten SSR markers, with the number of alleles per locus ranging from three (CPS103) to 24 alleles (CPS156) and a mean 9.2 alleles per locus (Table 1). Nei's gene diversity ( $H_{exp}$ ) varied from 0.52 (CPS159) to 0.88 (CPS156), with an average of 0.67. The evenness ( $E_5$ ) ranged from 0.57 (CPS140 and CPS159) to 0.87 (CPS103 and CPS161) with a mean of 0.73 (Table 1).

### 3.4 Genetic diversity

A total of 90 MLGs were detected among the 311 isolates. The genotype accumulation curve showed signs of a plateau at nine markers, suggesting that using ten SSR markers would be sufficient to detect the genotypic diversity of all isolates considered in this study (Supplementary

Fig. S1). Of the 90 MLGs detected, 49 MLGs were represented by only a single isolate and ten MLGs were shared between at least two populations (Fig. 2). The most dominant genotype (MLG.21) was identified in 28 isolates from seven populations, with the only exception being the 7HZ population. There were no shared MLGs between population 7HZ and the other populations (Fig. 2).

For genotypic diversity, the highest values ( $H = 2.795$ ,  $G = 12.721$ ) were observed for 1BH population and the lowest values ( $H = 1.660$ ,  $G = 3.380$ ) were observed for the 7HZ population. The genotypic evenness ( $E.5$ ) that measures the distribution of genotype in a population with  $E.5 > 0.5$  indicated an even distribution. The lowest  $E.5$  ( $E.5 = 0.720$ ) was found in the 7HZ population, and the highest ( $E.5 = 0.825$ ) was found in the 8HN population. Nei's unbiased gene diversity ( $H_{exp}$ ) for the eight geographically distributed populations varied from 0.485 to 0.636 (Table 2). The 1BH population had the highest gene diversity ( $H_{exp} = 0.636$ ), followed by the 2ZJA population ( $H_{exp} = 0.603$ ). The lowest gene diversity ( $H_{exp} = 0.485$ ) was observed in the 7HZ population.

### 3.5 Population structure

STRUCTURE analysis of 311 isolates suggested  $K = 2$  as the optimal number of clusters (Supplementary Fig. S2). Unlike other populations, almost all isolates in the 7HZ population were assigned to a single cluster (Fig. 3). A similar pattern was observed with DAPC where individuals from the 7HZ population formed a separate cluster, distinct from a cluster that included all isolates from the other populations (Fig. 4A). After removing the 7HZ population, further DAPC analysis was conducted using this dataset. This analysis revealed some level of sub-structure based on geography. Isolates from 2ZJA, 5QY, and 8HN populations formed three distinct clusters that could be differentiated from each other and from a fourth cluster composed of isolates from the remaining four populations (1BH, 3ZJB, 4YJ, and 6JM) (Fig. 4B).

### 3.6 Genetic differentiation

AMOVA showed a significant genetic differentiation among geographic populations ( $P \leq 0.001$ ) (Table 3). A higher genetic variation was observed within (86%) than among populations (14%), indicating a lower level of differentiation between populations. Similarly, analysis of population differentiation based on the pairwise comparisons of genetic differentiation ( $\phi_{PT}$ ) and gene flow

(Nm) also indicated a low-level genetic differentiation between populations (Table 4). The only exception was for the 7HZ population that had a higher level of genetic differentiation from all other populations. The highest genetic differentiation ( $\phi_{PT} = 0.290$ ) and the lowest gene flow ( $Nm = 1.222$ ) was observed between the 2ZJA and 7HZ populations. In contrast, the lowest genetic differentiation ( $\phi_{PT} = 0.017$ ) and the highest gene flow ( $Nm = 28.515$ ) was detected between 1BH and 3ZJB populations.

### 3.7 Reproductive mode

The index of association analysis ( $I_a$ ) for all populations based on clone-corrected datasets rejected the null hypothesis of random mating ( $P < 0.01$ , Table 5, Supplementary Fig. S3), suggesting that all populations were in linkage disequilibrium. The mating type idiomorphs were amplified for all 311 isolates (Table 5). The *MATI-1* mating type was dominant in all populations other than the 7HZ population where *MATI-2* was dominant. Only the *MATI-1* mating type was found in the 2ZJA population. Excluding the 8HN population ( $P = 0.61$ ), the ratios of *MATI-1* and *MATI-2* deviated significantly from the expected 1:1 ratio in a randomly mating population ( $P < 0.01$ , Table 5). These findings support a predominantly asexual mode of reproduction in the populations investigated.

## 4. Discussion

Ten polymorphic SSR markers were successfully developed for *C. pseudoreteaudii* using genome sequence data. These newly developed markers were used to genotype 311 isolates residing in eight geographically separated populations of the fungus from *Eucalyptus* plantations in southern China. The results showed that all but one of these populations had a high level of genetic diversity. Interestingly, an exception was found in population 7HZ that lacked a dominant genotype widely distributed across the other seven populations. This unusual population had a distinct structure and displayed a high level of genetic differentiation compared to other populations. Overall, unequal proportions of mating type with a high level of linkage disequilibrium suggests that asexual reproduction is the predominant mode of reproduction in the studied populations.

*Calonectria pseudoreteaudii* has caused severe disease outbreaks on *Eucalyptus* in plantations of southern China for at least 13 years since it was first discovered in 2010 (Lombard et al. 2010). Yet, this is the first study to use SSR markers to investigate the population biology of the pathogen from

this region or elsewhere. The pathogen was found to have a high level of genetic diversity, which is in contrast to a previous study where low levels of genetic diversity were found in samples from the same region when using phylogenetic markers (Wang and Chen 2020; Wu and Chen 2021). This result highlights the power of SSR markers compared to phylogenetic markers in studying pathogen populations. SSR markers have higher mutation rate compared to traditional phylogenetic markers, which leads to a greater level of polymorphism. This allows SSRs to detect more genetic variation and provide more sensitive measure of recent evolutionary events and population dynamics (Ellegren 2004; Schlotterer 2000). Phylogenetic markers often evolve more slowly and may not capture recent genetic changes, which are valuable when constructing evolutionary histories and seeking to understand deep genetic relationships (Patwardhan et al. 2014).

The fact that there were multiple shared MLGs and a high level of gene flow between populations suggests that there has been frequent movement of *C. pseudoreteaudii* between the different regions considered in this study. For example, a dominant genotype (MLG.21) was widely distributed in most of the populations. This is consistent with the results of studies on other *Calonectria* species, including for *C. ilicicola* (Wright et al. 2010), *C. pauciramosa* (Li et al. 2021), *C. pseudonaviculata* (Castroagudín et al. 2020), and *C. pteridis* (Freitas et al. 2019). The prevalence of a particular genotype in different regions would likely have arisen from the movement of infected plant germplasm among the regions (Burgess and Wingfield 2017), especially in non-native *Eucalyptus* in plantations, which are prone to an interchange of pathogens (Pérez et al. 2009).

Index of association and ratio of mating types supported a predominantly asexual reproductive cycle in the investigated populations of *C. pseudoreteaudii*. As in the case of most *Calonectria* species, the asexual *Cylindrocladium* state is predominantly found on infected tissues (Crous 2002), which would sustain a predominantly asexual life cycle such as that found in this study. The only exception was with the 8HN population that had a reasonably balanced distribution of *MAT1-1* and *MAT1-2* individuals. However, the index of association analyses still suggested that the genotypes observed in this population were most likely derived from asexual reproduction. The existence of both mating types in most populations of *C. pseudoreteaudii* provides for the possibility for sexual recombination, and even extremely rare sexual events would be capable of generating a high level of variation in a population (Bengtsson 2003). In turn, that would result in the emergence of new and possibly more aggressive genotypes that could then be distributed rapidly via asexual reproduction (McDonald and Linde 2002).

An interesting and unexpected result of this study was the discovery of a single population (7HZ) that was distinctly different from all others. The distinct nature of this population was clear based on its genetic differentiation [ $\phi$ PT (0.257-0.290)] and the DAPC result as it grouped in a single distinct cluster. The mating type of the isolates in this population were all of the *MATI-2* and thus different to the predominantly *MATI-1* mating type in all other populations. This difference could be explained in various ways. From a genetic point of view, the 7HZ population could have originated from a source population distinct from the others. The germplasm sources of *Eucalyptus* plantations in the sampling areas are unknown, suggesting that the 7HZ population of *C. pseudoreteaudii* may have been introduced via the introduction of *Eucalyptus* planting material (Wingfield et al. 2008, 2013). The germplasm carrying the pathogen could then contain specific pathogen genotypes, which would have led to genetic differences in the 7HZ population compared to other populations.

Another possible explanation for the origin of the distinct 7HZ population was that the isolates making up this population all originated from an area with a higher elevation 400 meters above sea level (MAS) as opposed to less than 100 MAS in the other populations. The altitude differences could provide a climatic and/or geographical condition that might lead to local adaptation, resulting in genetic divergence observed (Orsini et al. 2013). Another consideration was that the isolates in the 7HZ population were collected shortly after the area that was disturbed by a cyclone. This extreme disturbance could have led to the introduction of pathogens from unknown sources, which might also explain the genetic difference between the 7HZ and other populations.

Disease epidemics caused by invasive fungal pathogens often involve founder effects, where the invasion event is caused by a single or a limited number of pathogen genotypes (Drenth et al. 2019). The *C. pseudoreteaudii* populations investigated in this study did not show the typical characteristics of a new introduced pathogen that has low level genetic diversity (Gladieux et al. 2016). We therefore hypothesize that *C. pseudoreteaudii* populations studied have not been introduced from a single origin nor have arisen from a relatively recent invasion event. Other than those from China, there are only a few reports of disease caused by *C. pseudoreteaudii*; these being from India, Laos, and Vietnam (Bose et al. 2022; Crous et al. 2012; Phanthavong et al. 2023). Whether *C. pseudoreteaudii* originated in China or surrounding countries is unknown, but the overall results of this study suggest that it is a native pathogen in the region and where intermittent and localized outbreaks of disease occur where plants are susceptible and where the environment is conducive to infection.

The results of this study provide important foundational knowledge regarding the genetic diversity and population structure of *C. pseudoreteaudii*. They lay the groundwork to investigate the genetic variation of *C. pseudoreteaudii* populations in other countries and regions. These will also aid in tracking future pathways of dissemination of the pathogen. Future genomic studies on *C. pseudoreteaudii* should provide further insights into its ecological adaptations and infection biology, which will aid in predicting disease risks and facilitate the development of comprehensive disease management strategies to ensure the future health and sustainable development of *Eucalyptus* plantations.

### **Acknowledgements**

This study was supported by the Natural Science Foundation of Guangdong Province, China (Project No. 2022A1515010874), the National Key R&D Program of China (China-South Africa Forestry Joint Research Centre Project; project No. 2018YFE0120900), and the National Ten-thousand Talents Program (Project No. W03070115).

## Literature cited

- Afgan, E., Baker, D., van den Beek, M., Blankenberg, D., Bouvier, D., Čech, M., Chilton, J., Clements, D., Coraor, N., Eberhard, C., Grüning, B., Guerler, A., Hillman-Jackson, J., VonKuster, G., Rasche, E., Soranzo, N., Turaga, N., Taylor, J., Nekrutenko, A., and Goecks, J. 2016. The Galaxy platform for accessible, reproducible and collaborative biomedical analyses: 2016 update. *Nucleic Acids Res.* 44:W3–W10.
- Agapow, P. M., and Burt, A. Indices of multilocus linkage disequilibrium. *Mol. Ecol. Notes* 2001:1, 101102.
- Bengtsson, B. O. 2003. Genetic variation in organisms with sexual and asexual reproduction. *J. Evolution Biol.* 16:189–199.
- Billiard, S., López-Villavicencio, M., Hood, M. E., and Giraud, T. 2012. Sex, outcrossing and mating types: Unsolved questions in fungi and beyond. *J. Evolution Biol.* 25:1020–1038.
- Bolger, A. M., Lohse, M., and Usadel, B. 2014. Trimmomatic: A flexible trimmer for Illumina sequence data. *Bioinformatics* 30:2114–2120.
- Bose, R., Banerjee, S., Negi, N., Pandey, A., Bhandari, M. S., and Pandey, S. 2022. Identification and pathogenicity of *Calonectria pseudoreteauidii* causing leaf blight of *Eucalyptus* — a new record for India. *Physiol. Mol. Plant P.* 122:101917.
- Brown, A. H. D., Feldman, M. W., and Nevo, E. 1980. Multilocus structure of natural populations of *Hordeum spontaneum*. *Genetics* 96:523–536.
- Burgess, T. I., and Wingfield, M. J. 2017. Pathogens on the move: A 100-year global experiment with planted eucalypts. *BioScience* 67:14–25.
- Carbone, I., and Kohn, L. M. 1999. A method for designing primer sets for speciation studies in filamentous ascomycetes. *Mycologia* 91:553–556.
- Castroagudín, V. L., Weiland, J. E., Baysal-Gurel, F., Cubeta, M. A., Daughtrey, M. L., Gauthier, N. W., LaMondia, J., Luster, D. G., Hand, F. P., Shishkoff, N., Williams-Woodward, J., Yang, X., LeBlanc, N., and Crouch, J. A. 2020. One clonal lineage of *Calonectria pseudonaviculata* is primarily responsible for the boxwood blight epidemic in the United States. *Phytopathology* 110:1845–1853.
- Chen, C., Liang, X., Lin, Y., Hsiang, T., Xiang, M., and Zhang, Y. 2023. First report of leaf spot and stem blight on blueberry (*Vaccinium corymbosum* ‘Bluerain’) caused by *Calonectria pseudoreteauidii* in China. *Plant Dis.* 107:1951.
- Chen, S. F., Lombard, L., Roux, J., Xie, Y. J., Wingfield, M. J., and Zhou, X. 2011. Novel species

- of *Calonectria* associated with *Eucalyptus* leaf blight in southeast China. *Persoonia* 26:1–12.
- Coppin, E., Debuchy, R., Arnaise, S., and Picard, M. 1997. Mating types and sexual development in filamentous ascomycetes. *Microbiol. Mol. Biol. Rev.* 61:411–428.
- Crous P. W. 2002. Taxonomy and pathology of *Cylindrocladium* (*Calonectria*) and allied genera. American Phytopathological Society (APS Press), St. Paul, USA.
- Crous P. W., Groenewald, J. Z., Risède, J. M., Simoneau, P., and Hywel-Jones, N. L. 2004. *Calonectria* species and their *Cylindrocladium* anamorphs: Species with sphaeropedunculate vesicles. *Stud. Mycol.* 50:415–430.
- Crous P. W., Shivas, R. G., Wingfield, M. J., Summerell, B. A., Rossman, A. Y., Alves, J. L., Adams, G. C., Barreto, R. W., Bell, A., Coutinho, M. L., Flory, S. L., Gates, G., Grice, K. R., Hardy, G. E. St. J., Kleczewski, N. M., Lombard, L., Longa, C. M. O., Louis-Seize, G., Macedo, F., Mahoney, D. P., Maresi, G., Martin-Sanchez, P. M., Marvanová, L., Minnis, A. M., Morgado, L. N., Noordeloos, M. E., Phillips, A. J. L., Quaedvlieg, W., Ryan, P. G., Saiz-Jimenez, C., Seifert, K. A., Swart, W. J., Tan, Y. P., Tanney, J. B., Thu, P. Q., Videira, S. I. R., Walker, D. M., and Groenewald, J. Z. 2012. Fungal planet description sheets: 128–153. *Persoonia* 29:146–201.
- Crous P. W., Wingfield, M. J., Cheewangkoon, R., Carnegie, A. J., Burgess, T. I., Summerell, B. A., Edwards, J., Taylor, P. W. J., and Groenewald, J. Z. 2019. Foliar pathogens of eucalypts. *Stud. Mycol.* 94:125–298.
- Drenth, A., McTaggart, A. R., and Wingfield, B. D. 2019. Fungal clones win the battle, but recombination wins the war. *IMA Fungus* 10:18.
- Duong, T. A., De Beer, Z. W., Wingfield, B. D., and Wingfield, M. J. 2013. Characterization of the mating-type genes in *Leptographium procerum* and *Leptographium profanum*. *Fungal Biol.* 117:411–421.
- Earl, D. A., and vonHoldt, B. M. 2012. STRUCTURE HARVESTER: A website and program for visualizing STRUCTURE output and implementing the Evanno method. *Conserv. Genet. Resour.* 4:359–361.
- Ellegren, H. 2004. Microsatellites: simple sequences with complex evolution. *Nat. Rev. Genet.* 5:435–445.
- Engelbrecht, J., Duong, T.A. and Berg, N.v.d. 2017. New microsatellite markers for population studies of *Phytophthora cinnamomi*, an important global pathogen. *Sci Rep* 7:17631.
- Falush, D., Stephens, M., and Pritchard, J. K. 2003. Inference of population structure using multilocus genotype data: Linked loci and correlated allele frequencies. *Genetics* 164:1567–1587.
- Flutre, T., Duprat, E., Feuillet, C., and Quesneville, H. 2011. Considering transposable element

- diversification in de novo annotation approaches. PLoS ONE 6:e16526.
- Freitas, R. G., Alfenas, R. F., Guimarães, L. M. S., Badel, J. L., and Alfenas, A. C. 2019. Genetic diversity and aggressiveness of *Calonectria pteridis* in *Eucalyptus* spp. Plant Pathol. 68:869–877.
- Gladieux, P., Feurtey, A., Hood, M. E., Snirc, A., Clavel, J., Dutech, C., Roy, M., and Giraud, T. 2016. The population biology of fungal invasions. In *Invasion Genetics* (pp. 81–100). John Wiley and Sons, Ltd.
- Goodenough, U., and Heitman, J. 2014. Origins of eukaryotic sexual reproduction. CSH Perspect. Biol. 6:a016154.
- Grunwald, N. J., Goodwin, S. B., Milgroom, M. G., and Fry, W. E. 2003. Analysis of genotypic diversity data for populations of microorganisms. Phytopathology 93:738–746.
- Guindon, S., and Gascuel, O. 2003. A simple, fast, and accurate algorithm to estimate large phylogenies by maximum likelihood. Syst. Biol. 52:696–704.
- Highnam, G., Franck, C., Martin, A., Stephens, C., Puthige, A., Mittelman, D. 2013. Accurate human microsatellite genotypes from high-throughput resequencing data using informed error profiles. Nucleic Acids Res. 41:e32.
- Hollander, M., Wolfe, D. A., and Chicken, E. 2013. Nonparametric statistical methods. John Wiley & Sons, Hoboken, NJ.
- Jiang, G. Z., Gao, F., Yue, H., Tao, L., and He, X. Y. 2020. First report of fruit spot of *Macadamia* sp. caused by *Calonectria pentaseptata* in China. Plant Dis. 104:575.
- Jombart, T., Devillard, S., and Balloux, F. 2010. Discriminant analysis of principal components: A new method for the analysis of genetically structured populations. BMC Genet. 11:94.
- Kamvar, Z. N., Tabima, J. F., and Grünwald, N. J. 2014. *Poppr*: An R package for genetic analysis of populations with clonal, partially clonal, and/or sexual reproduction. PeerJ 2:e281.
- Katoh, K., and Standley, D. M. 2013. MAFFT multiple sequence alignment software version 7: Improvements in performance and usability. Mol. Biol. Evol. 30:772–780.
- Kearse, M., Moir, R., Wilson, A., Stones-Havas, S., Cheung, M., Sturrock, S., Buxton, S., Cooper, A., Markowitz, S., Duran, C., Thierer, T., Ashton, B., Meintjes, P., and Drummond, A. 2012. Geneious basic: An integrated and extendable desktop software platform for the organization and analysis of sequence data. Bioinformatics 28:1647–1649.
- Kopelman, N. M., Mayzel, J., Jakobsson, M., Rosenberg, N. A., and Mayrose, I. 2015. Clumpak: A program for identifying clustering modes and packaging population structure inferences across K. Mol. Ecol. Resour. 15:1179–1191.

- Langmead, B., and Salzberg, S. L. 2012. Fast gapped-read alignment with Bowtie 2. *Nat. Methods* 9:357–359.
- Li, J., Barnes, I., Liu, F., Wingfield, M. J., and Chen, S. F. 2021. Global genetic diversity and mating type distribution of *Calonectria pauciramosa*: An important wide-host-range plant pathogen. *Plant Dis.* 105:1648–1656.
- Li, J., Wingfield, B. D., Wingfield, M. J., Barnes, I., Fourie, A., Crous P. W., and Chen, S. F. 2020. Mating genes in *Calonectria* and evidence for a heterothallic ancestral state. *Persoonia* 45:163–176.
- Li, J., Wingfield, M. J., Barnes, I., and Chen, S. F. 2022. *Calonectria* in the age of genes and genomes: Towards understanding an important but relatively unknown group of pathogens. *Mol. Plant Pathol.* 23:1060–1072.
- Li, J., Wingfield, M. J., Liu, Q., Barnes, I., Roux, J., Lombard, L., Crous P. W., and Chen, S. F. 2017. *Calonectria* species isolated from *Eucalyptus* plantations and nurseries in South China. *IMA Fungus* 8:259–286.
- Li, W., Chen, S. F., Wingfield, M. J., and Duong, T. A. 2023a. *Calonectria queenslandica*: Causal agent of *Eucalyptus* leaf blight in southern China. *Plant Dis.* 107:730–742.
- Li, W., Chen, S. F., Wingfield, M. J., and Duong, T. A. 2023b. *Calonectria* species associated with diseased leaves and soils in southern China *Eucalyptus* plantations. *Phytopathology Research* 5:29.
- Liang, X., Wang, Q., and Chen, S. F. 2023. Phylogeny, morphology, distribution, and pathogenicity of seven *Calonectria* species from leaf blighted *Eucalyptus* in HaiNan Island, China. *Plant Dis.* 107:2579–2605.
- Liu, Q., Li, J., Wingfield, M. J., Duong, T. A., Wingfield, B. D., Crous P. W., and Chen, S. F. 2020. Reconsideration of species boundaries and proposed DNA barcodes for *Calonectria*. *Stud. Mycol.* 97:100106.
- Liu, Q., Wingfield, M. J., Duong, T. A., Wingfield, B. D., and Chen, S. F. 2022. Diversity and distribution of *Calonectria* species from plantation and forest soils in Fujian Province, China. *J Fungi* 8:811.
- Lombard, L., Zhou, X., Crous P. W., Wingfield, B. D., and Wingfield, M. J. 2010. *Calonectria* species associated with cutting rot of *Eucalyptus*. *Persoonia* 24:1–11.
- McDonald, B. A., and Linde, C. 2002. The population genetics of plant pathogens and breeding strategies for durable resistance. *Euphytica* 124:163–180.
- Nei, M. 1978. Estimation of average heterozygosity and genetic distance from a small number of

- individuals. *Genetics* 89:583–590.
- Nielsen, R., Tarpay, D. R., and Reeve, H. K. 2003. Estimating effective paternity number in social insects and the effective number of alleles in a population. *Mol. Ecol.* 12:3157–3164.
- O'Donnell, K., and Cigelnik, E. 1997. Two divergent intragenomic rDNA ITS2 types within a monophyletic lineage of the fungus *Fusarium* are nonorthologous. *Mol. Phylogenet. Evol.* 7:103–116.
- O'Donnell, K., Kistler, H. C., Cigelnik, E., and Ploetz, R. C. 1998. Multiple evolutionary origins of the fungus causing Panama disease of banana: Concordant evidence from nuclear and mitochondrial gene genealogies. *PNAS* 95:2044–2049.
- Old, K. M., Wingfield, M. J., and Yuan, Z. Q. 2003. A manual of diseases of *Eucalyptus* in South East Asia. CIFOR, Indonesia.
- Orsini, L., Vanoverbeke, J., Swillen, I., Mergeay, J., and De Meester, L. 2013. Drivers of population genetic differentiation in the wild: isolation by dispersal limitation, isolation by adaptation and isolation by colonization. *Mol. Ecol.* 22:5983–5999.
- Patwardhan, A., Ray, S., and Roy, A. 2014. Molecular markers in phylogenetic studies—a review. *J. Phylogenet. Evol. Biol.* 2:131.
- Peakall, R., and Smouse, P. E. 2012. GenAlEx 6.5: Genetic analysis in Excel. Population genetic software for teaching and research — an update. *Bioinformatics* 28:2537–2539.
- Pérez, G., Hunter, G.C., Slippers, B., Pérez, C., Wingfield, B. D., and Wingfield, M. J. 2009. *Teratosphaeria* (*Mycosphaerella*) *nubilosa*, the causal agent of *Mycosphaerella* leaf disease (MLD), recently introduced into Uruguay. *Eur. J. Plant Pathol.* 125:109–118.
- Phanthavong, S., Daly, A., Weir, B., Lee, D., Park, D., Balmas, V., and Burgess, L. 2023. First report of *Calonectria pseudoreteauidii* in Lao PDR associated with a leaf spot disease of *Macadamia integrifolia*. *Australas. Plant Path.* 52:23–26.
- Pritchard, J. K., Stephens, M., and Donnelly, P. 2000. Inference of population structure using multilocus genotype data. *Genetics* 155:945–959.
- Schlötterer, C. 2000. Evolutionary dynamics of microsatellite DNA. *Chromosoma* 109:365–371.
- Shannon, C. E. 2001. A mathematical theory of communication. *SIGMOBILE Mob. Comput. Commun. Rev.* 5:3–55.
- Stoddart, J. A., and Taylor, J. F. 1988. Genotypic diversity: Estimation and prediction in samples. *Genetics* 118:705–711.
- van Burik, J. A. H., Schreckhise, R. W., White, T. C., Bowden, R. A., and Myerson, D. 1998. Comparison of six extraction techniques for isolation of DNA from filamentous fungi. *Med.*

- Mycol. 36:299–303.
- Wang, Q., and Chen, S. F. 2020. *Calonectria pentaseptata* causes severe leaf disease of cultivated *Eucalyptus* on the Leizhou Peninsula of southern China. *Plant Dis.* 104:493–509.
- Wingfield, M. J., Brockerhoff, E. G., Wingfield, B. D., and Slippers, B. 2015. Planted forest health: The need for a global strategy. *Science* 349:832–836.
- Wingfield, M. J., Roux, J., Slippers, B., Hurley, B. P., Garnas, J., Myburg, A. A., and Wingfield, B. D. 2013. Established and new technologies reduce increasing pest and pathogen threats to *Eucalypt* plantations. *For. Ecol. Manage.* 301:35–42.
- Wingfield, M., Slippers, B., Hurley, B., Coutinho, T., Wingfield, B., and Roux, J. 2008. *Eucalypt* pests and diseases: Growing threats to plantation productivity. *Southern Forests* 70:139–144.
- Wright, L. P., Davis, A. J., Wingfield, B. D., Crous P. W., Brenneman, T., Wingfield, M. J. 2010. Population structure of *Cylindrocladium parasiticum* infecting peanuts (*Arachis hypogaea*) in Georgia, USA. *Eur. J. Plant Pathol.* 127:199–206.
- Wu, W., and Chen, S. F. 2021. Species diversity, mating strategy and pathogenicity of *Calonectria* species from diseased leaves and soils in the *Eucalyptus* plantation in southern China. *J. Fungi* 7:73.
- Wu, W., Li, W., Liu, F., and Chen, S. F. 2023. Evidence of high genetic diversity and differences in the population diversity of the *Eucalyptus* leaf blight pathogen *Calonectria pseudoreteaudii* from diseased leaves and soil in a plantation in Guangxi, China. *Microorganisms* 11:2785.
- Xie, Y., Arnold, R. J., Wu, Z., Chen, S., Du, A., and Luo, J. 2017. Advances in *eucalypt* research in China. *Front. Agr. Sci. Eng.* 4:380.
- Zhou, X. G. 2020. Loss estimates of *Eucalyptus* growth caused by leaf blight. *Agriculture and Technology* 40:91–92. (in Chinese)
- Zhu, J. H., Guo, W. S., Chen, H. M., Wu, J. Q., Chen, Q. Z., and Meng, X. M. 2011. Loss estimation of *Eucalyptus* growth caused by of *Eucalyptus* dieback. *Forest Pest and Disease* 5:6–10. (in Chinese)

## Figure legends

**Fig. 1.** Sampling sites of *Calonectria pseudoreteauidii* used in this study. A total of 311 isolates from eight geographic populations. Pie graph represents the number of isolates from each site.

**Fig. 2.** Multilocus genotypes (MLGs) found across eight populations of *Calonectria pseudoreteauidii*. A total of 90 MLGs were identified in the full datasets. Each bar represents a MLG where the high of the bar indicates the number of isolates. Different colors represent different populations, where the MLG comes from.

**Fig. 3.** Population structure ( $K = 2, 3,$  and  $4$ ) of *Calonectria pseudoreteauidii* isolates from eight populations. Each population is separated by a dashed black line and each bar corresponds to an individual MLG.

**Fig. 4.** Discriminant analysis of principal components (DAPC) calculated for (A) eight populations and (B) seven populations without the 7HZ population of *Calonectria pseudoreteauidii*. In the bottom left and bottom right corners, insets of the principal component analysis and discriminant analysis eigenvalues are shown, respectively.

**Supplementary Figure legends:**

**Supplementary Fig. S1.** The genotype accumulation curve of 311 *Calonectria pseudoreteauidii* isolates genotyped with 10 SSR primers. X-axis shows the number of loci sampled; Y-axis represents the number of MLGs observed in the dataset; red dashed line shows 100 % MLGs observed in this study.

**Supplementary Fig. S2.** The delta  $K$  analyzed by STRUCTURE HARVESTER showed a peak at  $K = 2$ .

**Supplementary Fig. S3.** Linkage disequilibrium testing ( $I_a$ ,  $P$ -values  $< 0.01$ ).

**Table 1.** Details of ten polymorphic SSR primers used for genotyping *C. pseudoreteaudii* isolates in this study.

SSR locus	Primer sequence (5' to 3')	T <sub>a</sub> (°C) <sup>a</sup>	Number of alleles	Repeat motif	Allele size (Genbank accession numbers)	Hexp <sup>b</sup>	E.5 <sup>c</sup>
CPS103	F: GGAGGAAGAGGGCACTAA R: CTTCTCCACTAGGCTGTT	52	3	(ACA) <sub>7, 9, 10</sub> <sup>d</sup>	277 <sup>e</sup> (PP827036), 283 (PP827037), 286 (PP827038)	0.58	0.87
CPS108	F: CTTGGGGTTTCTTCTTCTT R: AAATACGGTTGGTAGAGAG	52	6	(TTC) <sub>4, 9, 11, 12, 13, 14</sub>	258 (PP827039), 273 (PP827040), 279 (PP827041), 282 (PP827042), 285 (PP827043), 288 (PP827044)	0.70	0.80
CPS113	F: CGACTACAATCTGATGCAC R: CCAACGAAGACACGACAAA	52	7	(TTC) <sub>10, 11, 12, 13, 14, 15, 16</sub>	289 (PP827045), 292 (PP827046), 295 (PP827047), 298 (PP827048), 301 (PP827049), 304 (PP827050), 307 (PP827051)	0.71	0.77
CPS115	F: GAGATGAAAGAGGGGGAG R: AGGTGGGAATTGAAATGG	52	13	(CAA) <sub>11, 12, 13, 14, 15, 16, 20, 21, 23, 24, 26, 31, 32, 33, 34</sub>	381 (OQ865454), 384 (PP827052), 387 (PP827053), 390 (PP827054), 393 (PP827055), 396 (PP827056), 408 (PP827057), 411 (PP827058), 417 (PP827059), 420 (PP827060), 426 (PP827061), 444 (PP827062), 450 (PP827063)	0.75	0.65
CPS118	F: CGCAAAGTGTCTGGCTAA R: CGTGAGTGCTCCTAGTAA	52	12	(TCT) <sub>8, 12, 15, 16, 17, 18, 19, 21, 25, 26, 28, 29</sub>	356 (PP827064), 368 (PP827065), 377 (PP827066), 380 (PP827067), 383 (PP827068), 386 (PP827069), 389 (PP827070), 395 (PP827071), 407 (PP827072), 410 (PP827073), 416 (PP827074), 419 (PP827075)	0.81	0.83
CPS140	F: GACGCTAACACTGCTGCTA R: CCAAGATACTCCCTCACCAA	52	9	(TCG) <sub>6, 9, 11, 12, 14, 15, 16, 20, 21</sub>	340 (PP827076), 349 (PP827077), 355 (PP827078), 358 (PP827079), 364 (PP827080), 367 (PP827081), 370 (PP827082), 382 (PP827083), 385 (OQ865469)	0.55	0.57
CPS144	F: CGGGATAGCTATAGGAGGG R: CTGTCGGAGTTGGATCTG	52	7	(AAG) <sub>15, 17, 18, 19, 20, 21, 22</sub>	353 (PP827084), 359 (PP827085), 362 (PP827086), 365 (PP827087), 368 (PP827088), 371 (PP827089), 374 (PP827090)	0.59	0.66

CPS156	F: GGTGAAGTGGTTGATGAG	52	24	(GAAA) <sub>10</sub> , 12, 15, 16, 17, 18, 20, 21, 22, 23, 24, 25, 26, 27, 28, 32, 33, 35, 38, 42, 43,44, 46, 47	274 (PP827091), 282 (PP827092), 294 (PP827093), 298 (PP827094), 302 (PP827095), 306 (PP827096), 314 (PP827097), 318 (PP827098), 322 (PP827099), 326 (PP827100), 330 (PP827101), 334 (OQ865480), 338 (PP827102), 342 (PP827103), 346 (PP827104), 362 (PP827105), 366 (PP827106), 374 (PP827107), 386 (PP827108), 402 (PP827109), 406 (PP827110), 410 (PP827111), 418 (OQ865484), 422 (PP827112)	0.88	0.71
	R: AGAAATGTCGGTCTTGGT						
CPS159	F: ACCTCAGCGAAACCATAA	52	7	(AAG) <sub>5, 6, 10</sub> , 12, 13, 14, 15	353 (PP827113), 356 (PP827114), 368 (PP827115), 374 (PP827116), 377 (PP827117), 380 (PP827118), 383 (PP827119)	0.52	0.57
	R: GGGCATAATTTGTTGGGA						
CPS161	F: AATCTTGCACCTCTCCAC	52	4	(TATG) <sub>5,7</sub> , 8,9	435 (PP827120), 443 (PP827121), 447 (PP827122), 451 (OQ865492)	0.59	0.87
	R: GATCGACGCTACCAAAAC						

<sup>a</sup> Ta, annealing temperature.

<sup>b</sup> Hexp, Nei's unbiased gene diversity (Nei 1978).

<sup>c</sup> E.5, evenness (Grunwald et al. 2003).

<sup>d</sup> Numbers of SSR repeat motifs obtained in the sequences of 311 *C. pseudoreteaudii* isolates.

<sup>e</sup> Expected allele size.

**Table 2.** Genetic diversity statistics for *C. pseudoreteaudii* populations used in this study.

Population <sup>a</sup>	N <sup>b</sup>	Na <sup>c</sup>	Nef <sup>d</sup>	Hexp <sup>e</sup>	E.5 <sup>f</sup>	MLG <sup>g</sup>	eMLG <sup>h</sup>	H <sup>i</sup>	G <sup>j</sup>
1BH	64	50	3.090	0.636	0.800	23	13.328	2.795	12.721
2ZJA	32	40	2.607	0.603	0.790	14	11.584	2.341	8.127
3ZJB	30	37	2.343	0.563	0.770	10	8.728	1.847	4.455
4YJ	42	44	2.597	0.586	0.760	17	12.083	2.520	9.910
5QY	48	41	2.644	0.587	0.810	17	12.197	2.544	9.763
6JM	36	46	2.656	0.590	0.770	17	12.378	2.384	6.968
7HZ	36	32	2.118	0.485	0.720	9	7.505	1.660	3.580
8HN	23	32	2.462	0.555	0.825	10	10.000	2.209	8.397
Total	311	92	2.565	0.667	0.730	90	16.916	3.813	25.662

<sup>a</sup> 1BH: BeiHai; 2ZJA: LeiZhou, ZhanJiang; 3ZJB: MaZhang, ZhanJiang; 4YJ: YangJiang; 5QY: QingYuan; 6JM: JiangMen; 7HZ: HuiZhou; 8HN: HaiNan.

<sup>b</sup> N = Number of individuals.

<sup>c</sup> Na = Number of total alleles observed.

<sup>d</sup> Nef = Number of effective alleles (Nielsen et al. 2003).

<sup>e</sup> Hexp = Nei's unbiased gene diversity (Nei 1978).

<sup>f</sup> E.5 = Evenness.

<sup>g</sup> MLG = Number of multilocus genotypes (MLG) observed.

<sup>h</sup> eMLG = The number of expected MLG at the smallest sample size based on rarefaction.

<sup>i</sup> H = Shannon-Wiener Index of MLG diversity (Shannon 2001).

<sup>j</sup> G = Stoddart and Taylor's Index of MLG diversity (Stoddart and Taylor 1988).

**Table 3.** Analysis of molecular variance (AMOVA) of *C. pseudoreteaudii* isolates from eight geographic populations.

Source of variation	Degree of freedom	Sum of squares	Mean squares	Estimated variance	Percentage of total variation (%)	PhiPT value	P value <sup>a</sup>
Among populations	7	301.991	43.142	0.973	14%	0.143	0.001
Within populations	303	1765.295	5.826	5.826	86%		
Total	310	2067.286	6.669	6.799	100%		

<sup>a</sup>Level of significance was based on 999 random permutations.

**Table 4.** Population differentiation of all *C. pseudoreteaudii* populations examined in this study. Population differentiation ( $\phi_{PT}$ ) and gene flow (Nm) are presented below and above the diagonal, respectively.

	<b>1BH<sup>a</sup></b>	<b>2ZJA</b>	<b>3ZJB</b>	<b>4YJ</b>	<b>5QY</b>	<b>6JM</b>	<b>7HZ</b>	<b>8HN</b>
1BH	-	4.015	28.515	19.877	5.560	13.638	1.449	5.564
2ZJA	0.111	-	2.370	2.294	1.900	1.892	1.222	1.809
3ZJB	0.017	0.174	-	16.047	6.958	8.221	1.354	9.306
4YJ	0.025	0.179	0.030	-	3.796	4.971	1.258	4.804
5QY	0.083	0.208	0.067	0.116	-	4.782	1.417	3.795
6JM	0.035	0.209	0.057	0.091	0.095	-	1.281	4.796
7HZ	0.257	0.290	0.270	0.284	0.261	0.281	-	1.260
8HN	0.082	0.217	0.051	0.094	0.116	0.094	0.284	-

<sup>a</sup> 1BH: BeiHai; 2ZJA: LeiZhou, ZhanJiang; 3ZJB: MaZhang, ZhanJiang; 4YJ: YangJiang; 5QY: QingYuan; 6JM: JiangMen; 7HZ: HuiZhou; 8HN: HaiNan

**Table 5.** Recombination test and mating type ratios of *Calonectria pseudoreteaudii* examined in this study.

Population	Recombination test			Mating type ratio	
	$I_a^a$	$\bar{r}_d^b$	$P.I_a^c$	$MATI-1:MATI-2^d$	$P.\text{binom}^e$
1BH	0.999	0.11	0.001	51:13	0.01
2ZJA	1.234	0.14	0.001	27:5	0.01
3ZJB	1.887	0.21	0.001	30:0	0.01
4YJ	0.860	0.10	0.001	30:12	0.01
5QY	1.338	0.15	0.001	37:11	0.01
6JM	0.810	0.09	0.001	29:7	0.01
7HZ	1.440	0.16	0.001	4:32	0.01
8HN	0.685	0.08	0.004	14:9	0.61

<sup>a</sup>  $I_a$ , index of association (Brown et al. 1980) between loci.

<sup>b</sup>  $\bar{r}_d$ , standard  $I_a$  (Agapow and Burt 2001).

<sup>c</sup>  $P.I_a$ ,  $P$  values for index of association based on 1000 randomizations of the clone-corrected datasets.

<sup>d</sup> Mating type ratio was calculated using the number of *MATI-1* and *MATI-2* of individuals.

<sup>e</sup>  $P.\text{binom}$ , exact binomial test (Hollander et al. 2013) to determine whether the mating type frequencies significantly deviate from a 1:1 ratio.

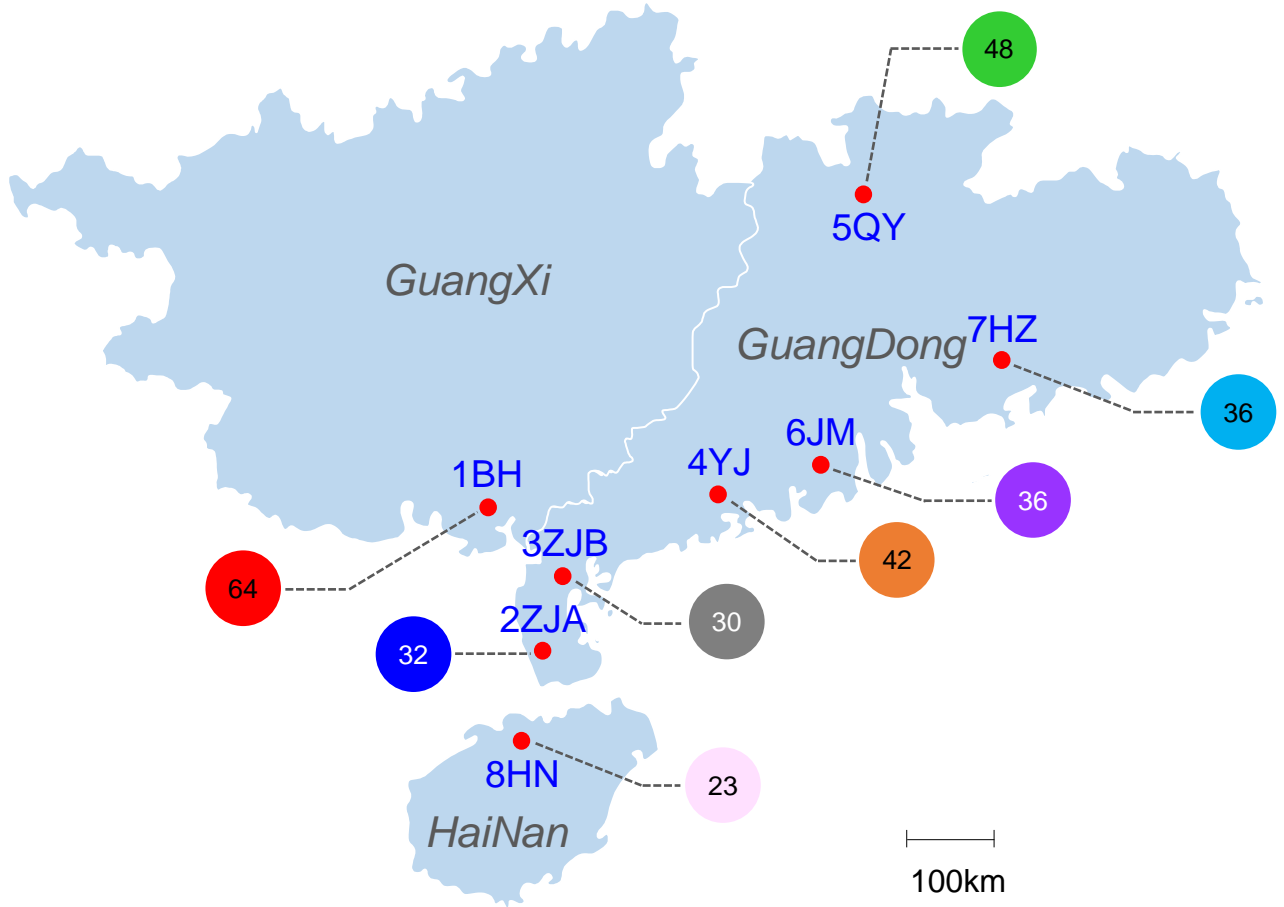


Fig. 1. Sampling sites of *Calonectria pseudoreteauidii* used in this study. A total of 311 isolates from eight geographic populations. Pie graph represents the number of isolates from each site.

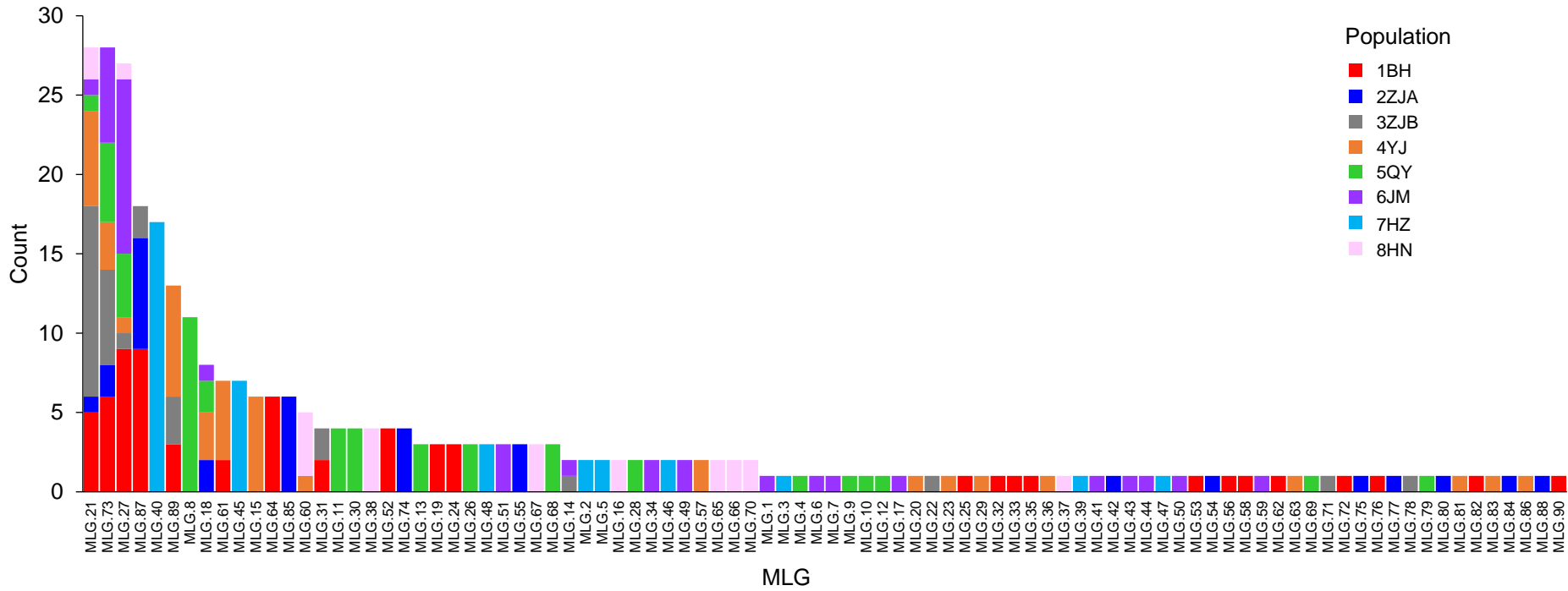


Fig. 2. Multilocus genotypes (MLGs) found across eight populations of *Calonectria pseudoreteauidii*. A total of 90 MLGs were identified in the full datasets. Each bar represents an MLG where the height of the bar indicates the number of isolates. Different colors represent different populations, where the MLG comes from.

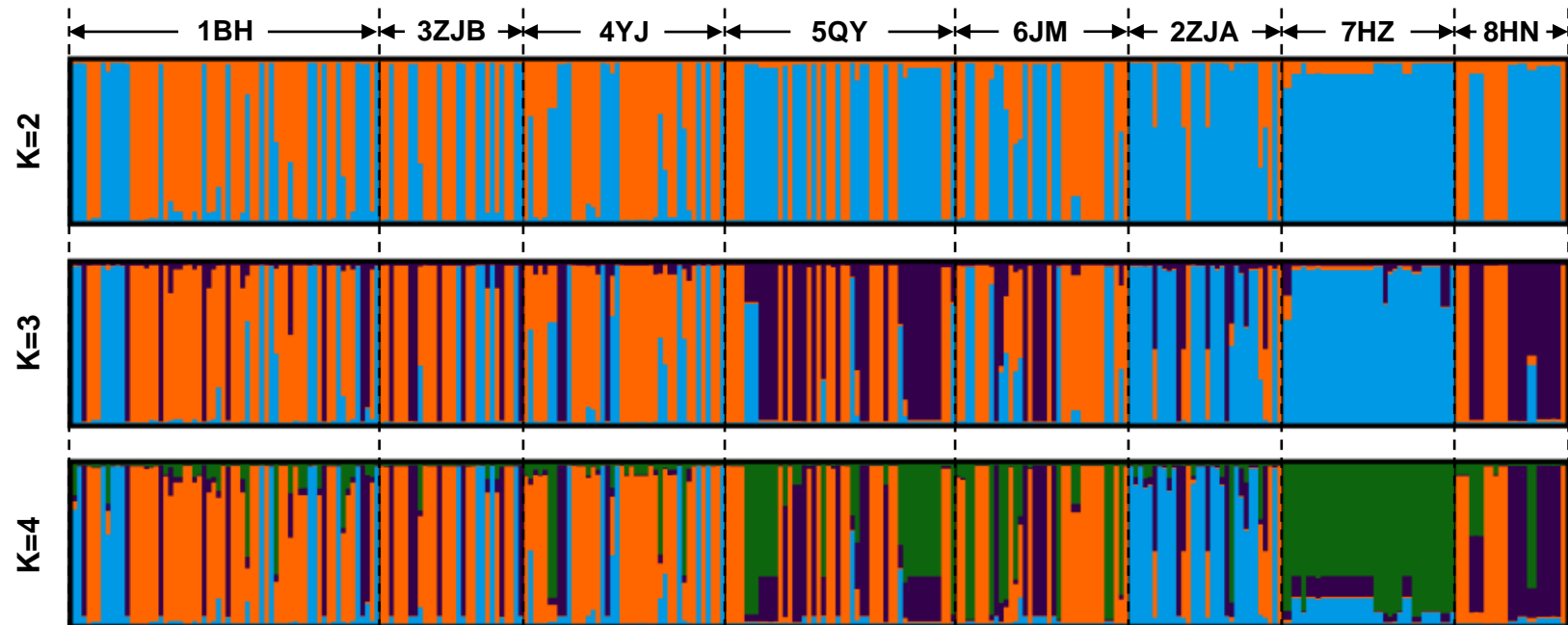


Fig. 3. Population structure (K = 2, 3, and 4) of *Calonectria pseudoreteaudii* isolates from eight populations. Each population is separated by a dashed black line and each bar corresponds to an individual multilocus genotype.

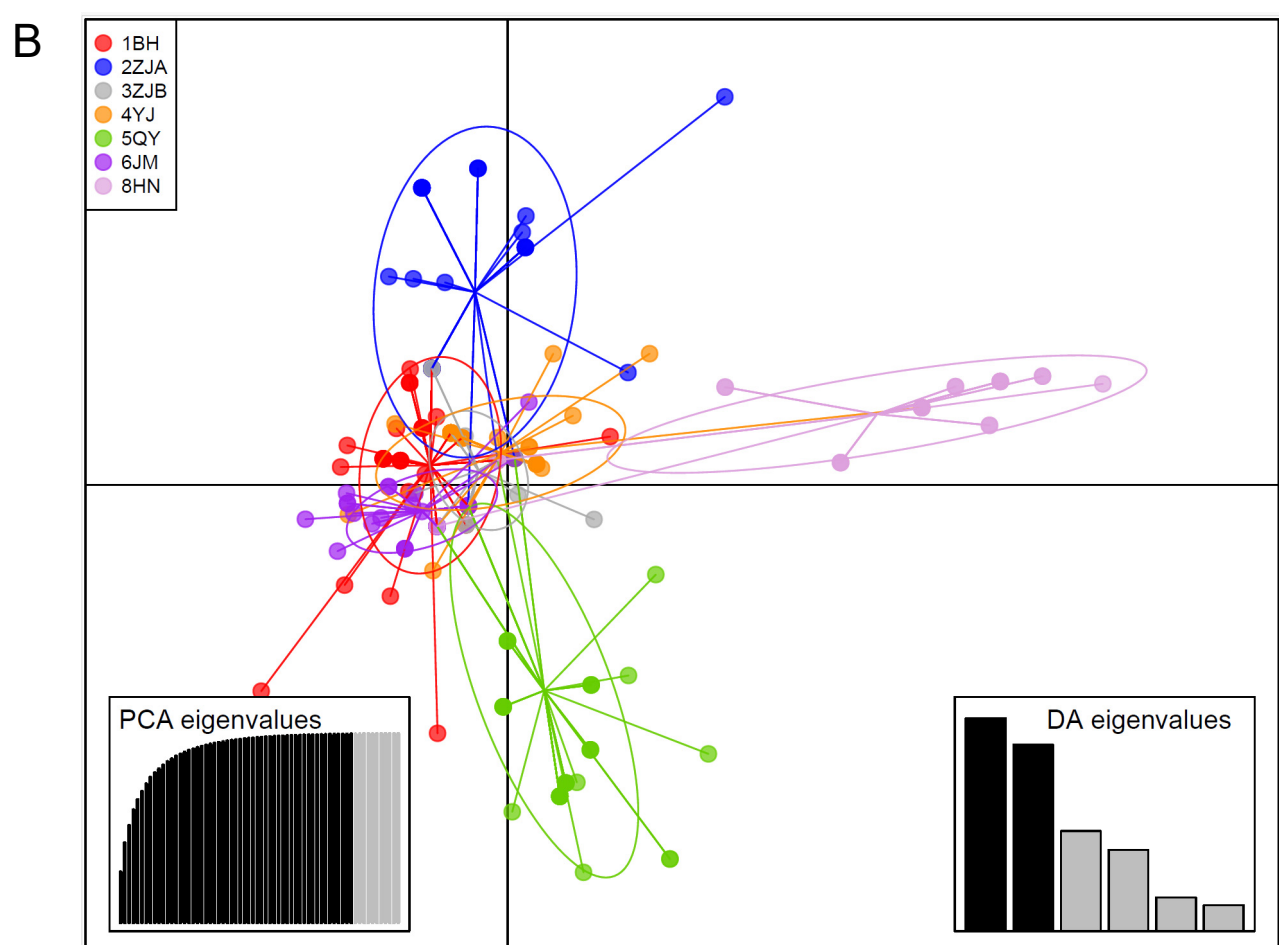
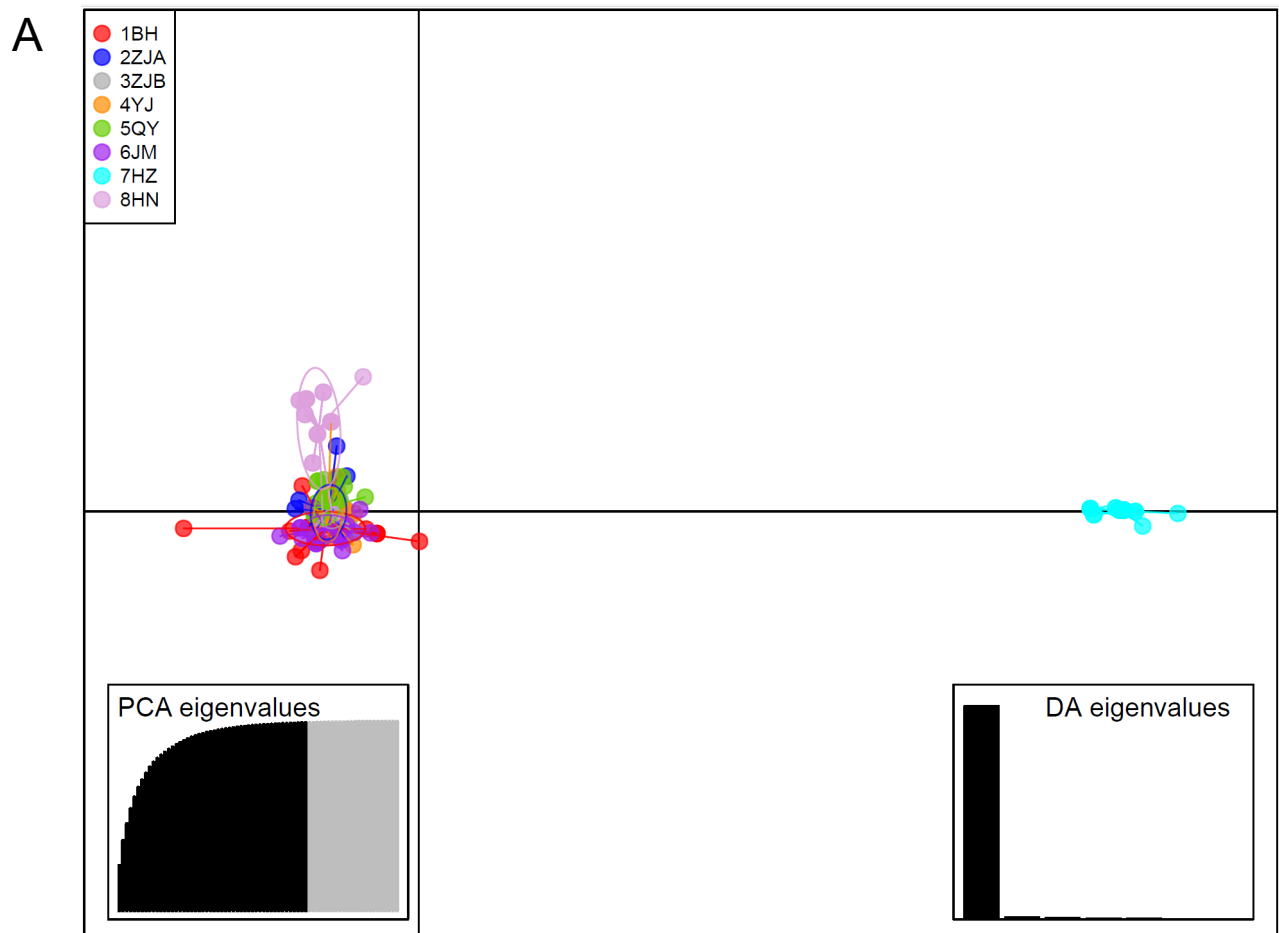


Fig. 4. Discriminant analysis of principal components calculated for A, eight populations and B, seven populations without the 7HZ population of *Calonectria pseudoreteauidii*. In the bottom left and bottom right corners, insets of the principal component analysis (PCA) and discriminant analysis (DA) eigenvalues are shown, respectively.

**Supplementary Table S1.** Isolates used in this study.

<b>Isolate number</b>	<b>Population code</b>	<b>Location</b>	<b>Host</b>	<b>Years</b>	<b>Collectors</b>	<b>Haplotype (<i>tef1_tub2</i>)</b>	<b>References</b>
CSF15861	1BH	BeiHai, GuangXi, China	<i>Eucalyptus</i>	2018	S.F. Chen, G.Q. Li and Q.C. Wang	11_11	Wu and Chen (2021)
CSF15865	1BH	BeiHai, GuangXi, China	<i>Eucalyptus</i>	2018	S.F. Chen, G.Q. Li and Q.C. Wang	11_11	Wu and Chen (2021)
CSF15866	1BH	BeiHai, GuangXi, China	<i>Eucalyptus</i>	2018	S.F. Chen, G.Q. Li and Q.C. Wang	11_11	Wu and Chen (2021)
CSF15877	1BH	BeiHai, GuangXi, China	<i>Eucalyptus</i>	2018	S.F. Chen, G.Q. Li and Q.C. Wang	11_11	Wu and Chen (2021)
CSF15879	1BH	BeiHai, GuangXi, China	<i>Eucalyptus</i>	2018	S.F. Chen, G.Q. Li and Q.C. Wang	11_11	Wu and Chen (2021)
CSF15881	1BH	BeiHai, GuangXi, China	<i>Eucalyptus</i>	2018	S.F. Chen, G.Q. Li and Q.C. Wang	11_11	Wu and Chen (2021)
CSF15882	1BH	BeiHai, GuangXi, China	<i>Eucalyptus</i>	2018	S.F. Chen, G.Q. Li and Q.C. Wang	11_11	Wu and Chen (2021)
CSF15886	1BH	BeiHai, GuangXi, China	<i>Eucalyptus</i>	2018	S.F. Chen, G.Q. Li and Q.C. Wang	11_11	Wu and Chen (2021)
CSF15887	1BH	BeiHai, GuangXi, China	<i>Eucalyptus</i>	2018	S.F. Chen, G.Q. Li and Q.C. Wang	11_11	Wu and Chen (2021)
CSF15888	1BH	BeiHai, GuangXi, China	<i>Eucalyptus</i>	2018	S.F. Chen, G.Q. Li and Q.C. Wang	11_11	Wu and Chen (2021)
CSF15892	1BH	BeiHai, GuangXi, China	<i>Eucalyptus</i>	2018	S.F. Chen, G.Q. Li and Q.C. Wang	11_11	Wu and Chen (2021)
CSF15901	1BH	BeiHai, GuangXi, China	<i>Eucalyptus</i>	2018	S.F. Chen, G.Q. Li and Q.C. Wang	11_11	Wu and Chen (2021)
CSF15903	1BH	BeiHai, GuangXi, China	<i>Eucalyptus</i>	2018	S.F. Chen, G.Q. Li and Q.C. Wang	11_11	Wu and Chen (2021)
CSF15906	1BH	BeiHai, GuangXi, China	<i>Eucalyptus</i>	2018	S.F. Chen, G.Q. Li and Q.C. Wang	11_11	Wu and Chen (2021)
CSF15908	1BH	BeiHai, GuangXi, China	<i>Eucalyptus</i>	2018	S.F. Chen, G.Q. Li and Q.C. Wang	11_11	Wu and Chen (2021)
CSF15910	1BH	BeiHai, GuangXi, China	<i>Eucalyptus</i>	2018	S.F. Chen, G.Q. Li and Q.C. Wang	11_11	Wu and Chen (2021)
CSF15912	1BH	BeiHai, GuangXi, China	<i>Eucalyptus</i>	2018	S.F. Chen, G.Q. Li and Q.C. Wang	11_11	Wu and Chen (2021)
CSF15913	1BH	BeiHai, GuangXi, China	<i>Eucalyptus</i>	2018	S.F. Chen, G.Q. Li and Q.C. Wang	11_11	Wu and Chen (2021)
CSF15914	1BH	BeiHai, GuangXi, China	<i>Eucalyptus</i>	2018	S.F. Chen, G.Q. Li and Q.C. Wang	11_11	Wu and Chen (2021)
CSF15916	1BH	BeiHai, GuangXi, China	<i>Eucalyptus</i>	2018	S.F. Chen, G.Q. Li and Q.C. Wang	11_11	Wu and Chen (2021)
CSF15919	1BH	BeiHai, GuangXi, China	<i>Eucalyptus</i>	2018	S.F. Chen, G.Q. Li and Q.C. Wang	11_11	Wu and Chen (2021)
CSF15922	1BH	BeiHai, GuangXi, China	<i>Eucalyptus</i>	2018	S.F. Chen, G.Q. Li and Q.C. Wang	11_11	Wu and Chen (2021)
CSF15925	1BH	BeiHai, GuangXi, China	<i>Eucalyptus</i>	2018	S.F. Chen, G.Q. Li and Q.C. Wang	11_11	Wu and Chen (2021)
CSF15927	1BH	BeiHai, GuangXi, China	<i>Eucalyptus</i>	2018	S.F. Chen, G.Q. Li and Q.C. Wang	11_11	Wu and Chen (2021)
CSF15933	1BH	BeiHai, GuangXi, China	<i>Eucalyptus</i>	2018	S.F. Chen, G.Q. Li and Q.C. Wang	11_11	Wu and Chen (2021)
CSF15936	1BH	BeiHai, GuangXi, China	<i>Eucalyptus</i>	2018	S.F. Chen, G.Q. Li and Q.C. Wang	11_11	Wu and Chen (2021)
CSF15939	1BH	BeiHai, GuangXi, China	<i>Eucalyptus</i>	2018	S.F. Chen, G.Q. Li and Q.C. Wang	11_11	Wu and Chen (2021)
CSF15942	1BH	BeiHai, GuangXi, China	<i>Eucalyptus</i>	2018	S.F. Chen, G.Q. Li and Q.C. Wang	11_11	Wu and Chen (2021)



CSF16039	1BH	BeiHai, GuangXi, China	<i>Eucalyptus</i>	2018	S.F. Chen, G.Q. Li and Q.C. Wang	11_11	Wu and Chen (2021)
CSF16042	1BH	BeiHai, GuangXi, China	<i>Eucalyptus</i>	2018	S.F. Chen, G.Q. Li and Q.C. Wang	11_11	Wu and Chen (2021)
CSF16045	1BH	BeiHai, GuangXi, China	<i>Eucalyptus</i>	2018	S.F. Chen, G.Q. Li and Q.C. Wang	11_11	Wu and Chen (2021)
CSF13337	2ZJA	LeiZhou, ZhanJiang, GuangDong, China	<i>Eucalyptus</i>	2018	S.F. Chen, Q.C. Wang, W.X. Wu and X. Yang	11_11	Wang and Chen (2020)
CSF13338	2ZJA	LeiZhou, ZhanJiang, GuangDong, China	<i>Eucalyptus</i>	2018	S.F. Chen, Q.C. Wang, W.X. Wu and X. Yang	11_11	this study
CSF13339	2ZJA	LeiZhou, ZhanJiang, GuangDong, China	<i>Eucalyptus</i>	2018	S.F. Chen, Q.C. Wang, W.X. Wu and X. Yang	11_11	this study
CSF13340	2ZJA	LeiZhou, ZhanJiang, GuangDong, China	<i>Eucalyptus</i>	2018	S.F. Chen, Q.C. Wang, W.X. Wu and X. Yang	11_11	Wang and Chen (2020)
CSF13342	2ZJA	LeiZhou, ZhanJiang, GuangDong, China	<i>Eucalyptus</i>	2018	S.F. Chen, Q.C. Wang, W.X. Wu and X. Yang	11_11	this study
CSF13343	2ZJA	LeiZhou, ZhanJiang, GuangDong, China	<i>Eucalyptus</i>	2018	S.F. Chen, Q.C. Wang, W.X. Wu and X. Yang	11_11	this study
CSF13344	2ZJA	LeiZhou, ZhanJiang, GuangDong, China	<i>Eucalyptus</i>	2018	S.F. Chen, Q.C. Wang, W.X. Wu and X. Yang	11_11	this study
CSF13345	2ZJA	LeiZhou, ZhanJiang, GuangDong, China	<i>Eucalyptus</i>	2018	S.F. Chen, Q.C. Wang, W.X. Wu and X. Yang	11_11	this study
CSF13346	2ZJA	LeiZhou, ZhanJiang, GuangDong, China	<i>Eucalyptus</i>	2018	S.F. Chen, Q.C. Wang, W.X. Wu and X. Yang	11_11	this study
CSF13347	2ZJA	LeiZhou, ZhanJiang, GuangDong, China	<i>Eucalyptus</i>	2018	S.F. Chen, Q.C. Wang, W.X. Wu and X. Yang	11_11	this study
CSF13349	2ZJA	LeiZhou, ZhanJiang, GuangDong, China	<i>Eucalyptus</i>	2018	S.F. Chen, Q.C. Wang, W.X. Wu and X. Yang	11_11	this study
CSF13350	2ZJA	LeiZhou, ZhanJiang, GuangDong, China	<i>Eucalyptus</i>	2018	S.F. Chen, Q.C. Wang, W.X. Wu and X. Yang	11_11	this study
CSF13351	2ZJA	LeiZhou, ZhanJiang, GuangDong, China	<i>Eucalyptus</i>	2018	S.F. Chen, Q.C. Wang, W.X. Wu and X. Yang	11_11	this study
CSF13352	2ZJA	LeiZhou, ZhanJiang, GuangDong, China	<i>Eucalyptus</i>	2018	S.F. Chen, Q.C. Wang, W.X. Wu and X. Yang	11_11	this study
CSF13353	2ZJA	LeiZhou, ZhanJiang, GuangDong, China	<i>Eucalyptus</i>	2018	S.F. Chen, Q.C. Wang, W.X. Wu and X. Yang	11_11	this study
CSF13354	2ZJA	LeiZhou, ZhanJiang, GuangDong, China	<i>Eucalyptus</i>	2018	S.F. Chen, Q.C. Wang, W.X. Wu and X. Yang	11_11	this study
CSF13356	2ZJA	LeiZhou, ZhanJiang, GuangDong, China	<i>Eucalyptus</i>	2018	S.F. Chen, Q.C. Wang, W.X. Wu and X. Yang	11_11	this study
CSF13357	2ZJA	LeiZhou, ZhanJiang, GuangDong, China	<i>Eucalyptus</i>	2018	S.F. Chen, Q.C. Wang, W.X. Wu and X. Yang	11_11	this study

CSF13358	2ZJA	LeiZhou, ZhanJiang, GuangDong, China	<i>Eucalyptus</i>	2018	S.F. Chen, Q.C. Wang, W.X. Wu and X. Yang	11_11	this study
CSF13359	2ZJA	LeiZhou, ZhanJiang, GuangDong, China	<i>Eucalyptus</i>	2018	S.F. Chen, Q.C. Wang, W.X. Wu and X. Yang	11_11	this study
CSF13360	2ZJA	LeiZhou, ZhanJiang, GuangDong, China	<i>Eucalyptus</i>	2018	S.F. Chen, Q.C. Wang, W.X. Wu and X. Yang	11_11	this study
CSF13361	2ZJA	LeiZhou, ZhanJiang, GuangDong, China	<i>Eucalyptus</i>	2018	S.F. Chen, Q.C. Wang, W.X. Wu and X. Yang	11_11	Wang and Chen (2020)
CSF13362	2ZJA	LeiZhou, ZhanJiang, GuangDong, China	<i>Eucalyptus</i>	2018	S.F. Chen, Q.C. Wang, W.X. Wu and X. Yang	11_11	Wang and Chen (2020)
CSF13364	2ZJA	LeiZhou, ZhanJiang, GuangDong, China	<i>Eucalyptus</i>	2018	S.F. Chen, Q.C. Wang, W.X. Wu and X. Yang	11_11	this study
CSF13365	2ZJA	LeiZhou, ZhanJiang, GuangDong, China	<i>Eucalyptus</i>	2018	S.F. Chen, Q.C. Wang, W.X. Wu and X. Yang	11_11	this study
CSF13366	2ZJA	LeiZhou, ZhanJiang, GuangDong, China	<i>Eucalyptus</i>	2018	S.F. Chen, Q.C. Wang, W.X. Wu and X. Yang	11_11	this study
CSF13367	2ZJA	LeiZhou, ZhanJiang, GuangDong, China	<i>Eucalyptus</i>	2018	S.F. Chen, Q.C. Wang, W.X. Wu and X. Yang	11_11	this study
CSF13368	2ZJA	LeiZhou, ZhanJiang, GuangDong, China	<i>Eucalyptus</i>	2018	S.F. Chen, Q.C. Wang, W.X. Wu and X. Yang	11_11	this study
CSF13369	2ZJA	LeiZhou, ZhanJiang, GuangDong, China	<i>Eucalyptus</i>	2018	S.F. Chen, Q.C. Wang, W.X. Wu and X. Yang	11_11	this study
CSF13370	2ZJA	LeiZhou, ZhanJiang, GuangDong, China	<i>Eucalyptus</i>	2018	S.F. Chen, Q.C. Wang, W.X. Wu and X. Yang	11_11	this study
CSF13371	2ZJA	LeiZhou, ZhanJiang, GuangDong, China	<i>Eucalyptus</i>	2018	S.F. Chen, Q.C. Wang, W.X. Wu and X. Yang	11_11	this study
CSF13372	2ZJA	LeiZhou, ZhanJiang, GuangDong, China	<i>Eucalyptus</i>	2018	S.F. Chen, Q.C. Wang, W.X. Wu and X. Yang	11_11	this study
CSF13040	3ZJB	MaZhang, ZhanJiang, GuangDong, China	<i>Eucalyptus</i>	2018	S.F. Chen, Q.C. Wang, W.X. Wu, X. Yang and L.L. Liu	11_11	Wang and Chen (2020)
CSF13045	3ZJB	MaZhang, ZhanJiang, GuangDong, China	<i>Eucalyptus</i>	2018	S.F. Chen, Q.C. Wang, W.X. Wu, X. Yang and L.L. Liu	11_11	Wang and Chen (2020)
CSF13049	3ZJB	MaZhang, ZhanJiang, GuangDong, China	<i>Eucalyptus</i>	2018	S.F. Chen, Q.C. Wang, W.X. Wu, X. Yang and L.L. Liu	11_11	this study
CSF13052	3ZJB	MaZhang, ZhanJiang, GuangDong, China	<i>Eucalyptus</i>	2018	S.F. Chen, Q.C. Wang, W.X. Wu, X. Yang and L.L. Liu	11_11	this study
CSF13056	3ZJB	MaZhang, ZhanJiang, GuangDong, China	<i>Eucalyptus</i>	2018	S.F. Chen, Q.C. Wang, W.X. Wu, X. Yang and L.L. Liu	11_11	this study
CSF13061	3ZJB	MaZhang, ZhanJiang, GuangDong, China	<i>Eucalyptus</i>	2018	S.F. Chen, Q.C. Wang, W.X. Wu, X. Yang and L.L. Liu	11_11	this study













CSF12355	7HZ	HuiZhou, GuangDong, China	<i>Eucalyptus</i>	2018	S.F. Chen, G.Q. Li and W.W. Li	11_11	Li et al. (2023b)
CSF12356	7HZ	HuiZhou, GuangDong, China	<i>Eucalyptus</i>	2018	S.F. Chen, G.Q. Li and W.W. Li	11_11	Li et al. (2023b)
CSF12362	7HZ	HuiZhou, GuangDong, China	<i>Eucalyptus</i>	2018	S.F. Chen, G.Q. Li and W.W. Li	11_11	Li et al. (2023b)
CSF17074	8HN	LinGao, HaiNan, China	<i>Eucalyptus</i>	2019	S.F. Chen, W. Wang, W.X. Wu, L.L. Liu, F. Chen and Y.X. Zheng	11_11	this study
CSF17077	8HN	LinGao, HaiNan, China	<i>Eucalyptus</i>	2019	S.F. Chen, W. Wang, W.X. Wu, L.L. Liu, F. Chen and Y.X. Zheng	11_11	this study
CSF17081	8HN	LinGao, HaiNan, China	<i>Eucalyptus</i>	2019	S.F. Chen, W. Wang, W.X. Wu, L.L. Liu, F. Chen and Y.X. Zheng	11_11	this study
CSF17084	8HN	LinGao, HaiNan, China	<i>Eucalyptus</i>	2019	S.F. Chen, W. Wang, W.X. Wu, L.L. Liu, F. Chen and Y.X. Zheng	11_11	this study
CSF17087	8HN	LinGao, HaiNan, China	<i>Eucalyptus</i>	2019	S.F. Chen, W. Wang, W.X. Wu, L.L. Liu, F. Chen and Y.X. Zheng	11_11	this study
CSF17090	8HN	LinGao, HaiNan, China	<i>Eucalyptus</i>	2019	S.F. Chen, W. Wang, W.X. Wu, L.L. Liu, F. Chen and Y.X. Zheng	11_11	this study
CSF17093	8HN	LinGao, HaiNan, China	<i>Eucalyptus</i>	2019	S.F. Chen, W. Wang, W.X. Wu, L.L. Liu, F. Chen and Y.X. Zheng	11_11	this study
CSF17096	8HN	LinGao, HaiNan, China	<i>Eucalyptus</i>	2019	S.F. Chen, W. Wang, W.X. Wu, L.L. Liu, F. Chen and Y.X. Zheng	11_11	this study
CSF17099	8HN	LinGao, HaiNan, China	<i>Eucalyptus</i>	2019	S.F. Chen, W. Wang, W.X. Wu, L.L. Liu, F. Chen and Y.X. Zheng	11_11	this study
CSF21460	8HN	LinGao, HaiNan, China	<i>Eucalyptus</i>	2020	S.F. Chen and Q.C. Wang	11_11	Liang et al. (2023)
CSF21461	8HN	LinGao, HaiNan, China	<i>Eucalyptus</i>	2020	S.F. Chen and Q.C. Wang	11_11	Liang et al. (2023)
CSF21474	8HN	LinGao, HaiNan, China	<i>Eucalyptus</i>	2020	S.F. Chen and Q.C. Wang	11_11	Liang et al. (2023)
CSF21475	8HN	LinGao, HaiNan, China	<i>Eucalyptus</i>	2020	S.F. Chen and Q.C. Wang	11_11	Liang et al. (2023)
CSF21496	8HN	LinGao, HaiNan, China	<i>Eucalyptus</i>	2020	S.F. Chen and Q.C. Wang	11_11	Liang et al. (2023)
CSF21497	8HN	LinGao, HaiNan, China	<i>Eucalyptus</i>	2020	S.F. Chen and Q.C. Wang	11_11	this study
CSF21521	8HN	LinGao, HaiNan, China	<i>Eucalyptus</i>	2020	S.F. Chen and Q.C. Wang	11_11	this study
CSF21522	8HN	LinGao, HaiNan, China	<i>Eucalyptus</i>	2020	S.F. Chen and Q.C. Wang	11_11	Liang et al. (2023)
CSF21531	8HN	LinGao, HaiNan, China	<i>Eucalyptus</i>	2020	S.F. Chen and Q.C. Wang	11_11	Liang et al. (2023)
CSF21532	8HN	LinGao, HaiNan, China	<i>Eucalyptus</i>	2020	S.F. Chen and Q.C. Wang	11_11	Liang et al. (2023)
CSF21534	8HN	LinGao, HaiNan, China	<i>Eucalyptus</i>	2020	S.F. Chen and Q.C. Wang	11_11	this study
CSF21543	8HN	LinGao, HaiNan, China	<i>Eucalyptus</i>	2020	S.F. Chen and Q.C. Wang	11_11	this study
CSF21544	8HN	LinGao, HaiNan, China	<i>Eucalyptus</i>	2020	S.F. Chen and Q.C. Wang	11_11	this study
CSF21567	8HN	LinGao, HaiNan, China	<i>Eucalyptus</i>	2020	S.F. Chen and Q.C. Wang	11_11	this study

**Supplementary Table S2.** Details of 38 polymorphic SSR markers developed in this study.

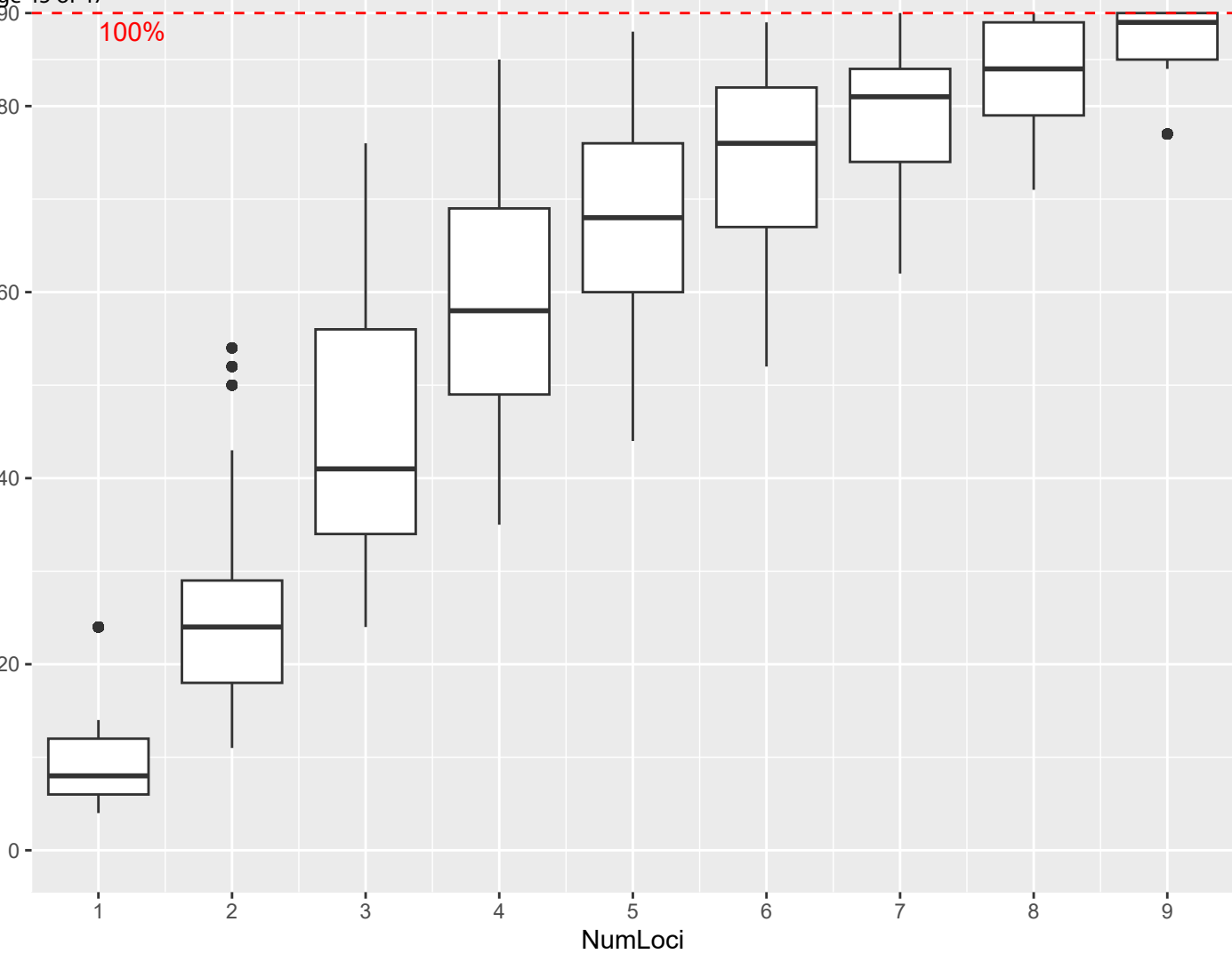
SSR Locus	Motif type	Sequence Fwd	GC content Fwd	Melt. temp. Fwd	Sequence Rev	GC content Rev	Melt. temp. Rev
CPS101	GAG	GGAAGAGCATGAAGGAGT	0.5	56.33	GGCGATCGTAGCTGAAGA	0.56	56.01
CPS103	ACA	GGAGGAAGAGGGCACTAA	0.56	55.89	CTTCTCCACTAGGCTGTT	0.5	55.33
CPS105	AGA	GATGCTGGAGACGACGTA	0.56	55.8	CTCTCACTCACTCTCACT	0.5	55.97
CPS108	TTC	CTTGGGGTTTCTTCTTCTT	0.42	54.25	AAATACGGTTGGTAGAGAG	0.42	53.69
CPS109	AAG	GTCCTCCCACATCTACATT	0.47	56.09	CTCACCATTTTCATCCGCA	0.5	55.77
CPS111	AGA	CGAAAGAAGACGGACTAGA	0.47	54.54	TGGCTGAGATGGAATTTG	0.44	54.27
CPS112	CCT	CGTGTTAGTTGATGTTATGG	0.4	53.47	GGAGGGTGAAGAGATGGA	0.56	53.17
CPS113	TTC	CGACTACAATCTGATGCAC	0.47	55.17	CCAACGAAGACACGACAAA	0.47	55.29
CPS115	CAA	GAGATGAAAGAGGGGGAG	0.56	54.33	AGGTGGGAATTGAAATGG	0.44	54.34
CPS117	CTTT	CCCCGCAATCTATTATCT	0.44	52.73	CATTCTCGCATATACCCA	0.44	52.94
CPS118	TCT	CGCAAAGTGCTGGCTAA	0.5	55.83	CGTGAGTGCTCCTAGTAA	0.5	56.38
CPS120	TGC	GAGAGGAAACATGCCCGA	0.56	55.85	GATGACGATGACCGCAGA	0.56	55.24
CPS126	TTA	CACTGTGGCTATCTTCCT	0.5	55.62	TCACGGCGACATTTTCTT	0.44	55.92
CPS128	CGA	CTACGGCTCCAACAAGAA	0.5	53.51	ACACCGTCAAAGTACACA	0.44	53.63
CPS129	GGC	GAATAAGGAGGTGGCGGA	0.56	56.48	CCTGATTGTGCCTCTGATT	0.47	56.82
CPS131	GGA	ACCAACAATACCAAGCAC	0.44	55.23	GGAGTAGTCTGGAGGTATG	0.53	54.45
CPS133	GAG	TATCGAGACGGTTGACCT	0.5	56.81	GAACTGGATGATGGCTGC	0.56	56.57
CPS135	AAC	AGACATCCTCACTCCCAC	0.56	57.72	TTCATCCTTCTCGGCCTT	0.5	57.7
CPS139	CCT	GCATGGGTGATTGTGATAGA	0.45	55.84	GAGGAATGAAAATGGAGGAG	0.45	55.64
CPS140	TCG	GACGCTAACACTGCTGCTA	0.53	57.04	CCAAGATACTCCCTCACCAA	0.5	57.01
CPS143	TTG	CTGTTTATGGGCATTGCATT	0.4	56.62	GTTTGTGGTGTGATGGG	0.5	56.46
CPS144	AAG	CGGGATAGCTATAGGAGGG	0.58	56.37	CTGTCCGAGTTGGATCTG	0.56	56.34
CPS146	CTC	AACCATCATCTTACTCTCTC	0.4	53.43	TTTCAGTCACTTCTCCACA	0.42	53.43
CPS147	GAC	CTGAGCAAGAAGACCGAA	0.5	56.13	TGCAAACCAACCTGACGA	0.5	55.08
CPS148	GCT	CTGCTGAACCAATTCTCT	0.44	54.26	CCTCATGCTCGAAAATCT	0.44	54.18
CPS150	TTTC	GGAGAGGAAGAAGACCAG	0.56	53.94	GAATCAAATCATGACGACC	0.42	53.6
CPS151	GAG	TGTCACTCTTTTCCGTCT	0.44	54.54	GATCAATCTCGAAGCCAC	0.5	54.38

CPS152	AAC	GTGGGAGACTTGTAGATGG	0.53	56.15	GAATATTGTGTCTGCACGG	0.47	56.09
CPS153	TCGC	CGAGCAATGATACCTACAA	0.42	52.61	GACAAACGAGAATTGAGGA	0.42	52.67
CPS155	ACC	AGAGGGAGATGGGAAATG	0.5	55.71	GCTAGGGCAAGTACGATT	0.5	55.24
CPS156	GAAA	GGTGAAGTGTTGATGAG	0.5	55.84	AGAAATGTCGGTCTTGGT	0.44	56.21
CPS157	CCT	CGGCATCGTATTGTCACT	0.5	56.73	CCGCTCCTGATTCACTTT	0.5	56.97
CPS158	CTT	ATGCTATACGAGGCAGAA	0.44	55.14	GTGGAGAGGGAGGTAATG	0.56	55.83
CPS159	AAG	ACCTCAGCGAAACCATAA	0.44	55.92	GGGCATAATTTGTTGGGA	0.44	55.11
CPS160	CTG	TAACCTAGTGAGGCGGGA	0.56	55.78	CTATGAGTTGCCGTTGA	0.5	55.33
CPS161	TATG	AATCTTGACCTCTCCAC	0.5	55.9	GATCGACGCTACCAAAAC	0.5	55.98
CPS162	TGT	CATTTCTTGCACTCGCTT	0.44	55.75	GGGTTAGACGAGTAGGATT	0.45	55.92
CPS163	TGC	AGAAACCGGAGAGAAAAG	0.44	54.61	GGCAAAGAAAAAGGTCAAG	0.42	55.55

---

100%

MLG



$$\text{DeltaK} = \text{mean}(|L''(K)|) / \text{sd}(L(K))$$

